Contents lists available at ScienceDirect

Molecular Phylogenetics and Evolution

Morphological, molecular and biogeographic evidence support two new species in the *Uroptychus naso* complex (Crustacea: Decapoda: Chirostylidae)

Gary C.B. Poore [a,*], Nikos Andreakis [b]

[a] Museum Victoria, GPO Box 666, Melbourne, Vic. 3000, Australia
[b] Australian Institute of Marine Science, PMB No. 3, Townsville, QLD 4810, Australia

ARTICLE INFO

ABSTRACT

The tropical to subtropical squat lobster *Uroptychus naso* Van Dam, 1933 (Chirostylidae) is a widely distributed species originally described from Indonesia, subsequently reported from the Philippines, Taiwan, Japan and it has recently been discovered on the continental slope of north-western Australia. Populations of *U. naso* occur along the Indo-Pacific Ocean continental margin crossing the recently proposed marine analog of Wallace's line, responsible for past population fragmentation and ancient speciation. Sequence data from mitochondrial (COI, 16S) and nuclear (H3) DNA regions were used to assess genealogical relationships among geographically disjoint populations of the species throughout its known distribution range. Several mitochondrial lineages, corresponding to geographically isolated populations and three cryptic species were encountered, namely, *U. naso* sensu stricto and two new species, *Uroptychus cyrano* and *Uroptychus pinocchio* spp. nov. *U. pinocchio* is encountered only in Japan, Taiwan and the Philippines; *U. cyrano* is confined to north-western Australia; and *U. naso* consists of three genetically distinct populations distributed on both sides of the marine Wallace's line. Fossil-calibrated divergence time approximations indicated a most recent common ancestor (MRCA) for *U. naso* and *U. cyrano* from early Eocene whilst northern and southern populations of the former have been separated probably since the Miocene. These patterns may represent a standard distribution trend for several other deep-sea invertebrate species with similar geographical ranges.

1. Introduction

Molecular phylogenetics and systematics have greatly improved our understanding of marine diversity thereby allowing for a broader perception of morphological character evolution and delineation of species, the latter essential for biodiversity estimates. This is most important in marine invertebrates with so-called wide geographical distribution ranges but which prove to comprise morphologically cryptic species or species complexes (Caputi et al., 2007; Knowlton, 1986; Machordom and Macpherson, 2004; Seidel et al., 2009).

Squat lobsters of the families Chirostylidae, Galatheidae, Munididae and Munidopsidae (Baba et al., 2008; Taylor et al., 2010) are found in all oceans, typically associated with coral assemblages in deep-sea waters from continental slopes to abyssal depths. Species encountered in the Southwest Pacific (SWP) for instance, are hypothesised to be the result of a relatively old explosive radiation event followed by morphological stasis (Machordom and Macpherson, 2004). This hypothesis is now being tested by a large-scale comparative phylogeographic survey that incorporates recent collections of squat lobsters from north-western Australia (NWA) combined with previously described taxa of SWP origin (Australia's Marine Biodiversity Hub – http://www.marinehub.org/index.php/site/home/). The Chirostylidae comprise seven genera and 192 described species. Of these, *Uroptychus* represents the most species-rich genus with 124 described species (Baba et al., 2008) and perhaps 70 more yet to be described (K. Baba, pers. comm.). Amongst these species, individuals of *Uroptychus naso* Van Dam, 1933 are distinctive with a particularly long broad rostrum, several prominent lateral carapace spines and tuberculate dorsal carapace. The species was described from the Kei Islands (Indonesia) and subsequently populations were reported throughout the western Pacific (WP) archipelago in Indonesia, the Philippines, Taiwan and Japan (Baba et al., 2008 and references therein). Recently collected material from the continental slope of NWA was tentatively identified as belonging to this species.

The distribution range of *U. naso* overlaps the contact zone between the Indian and the Pacific Oceans and is typical of many marine species exhibiting geographically associated genetic discontinuities (de Bruyn et al., 2004; Lourie and Vincent, 2004; Williams et al., 2002). The collision between Asian and Australasian plates during the Miocene and the separation of the Indian and the Pacific basins during the Pleistocene represent a

* Corresponding author.
E-mail address: gpoore@museum.vic.gov.au (G.C.B. Poore).

major biogeographical barrier between populations and sister taxa in the Indian and Pacific Oceans. On the other hand, the Indo-Pacific break (IPB) is nearly perpendicular to Wallace's line. The latter is an alternative biogeographical boundary, hypothesised to be responsible for the separation of terrestrial flora and fauna of eastern Asian and Australasian origins (Barber et al., 2000, 2002; Lourie and Vincent, 2004; Porter, 1989; Williams et al., 2002).

Preliminary molecular analyses from NWA specimens identified as *U. naso* indicated that two distinct mitochondrial lineages occur sympatrically. This result raised the question of the identity or identities of this species throughout its distribution range. Given the reported distribution of *U. naso*, we regard this species as an excellent model system to test the impact of the IPB and the marine Wallace's line.

Our material from NW Australia was supplemented by fresh material from throughout the species' range in the NW Pacific and compared with most of the specimens previously reported and now in museums. Importantly, the morphology of all specimens was compared with that of the type specimens. Mitochondrial and nuclear coding regions together with ribosomal genes have been valuable tools in inferring phylogenies, reconstructing genealogies, corroborating morphological systematics and uncovering speciation patterns in decapod crustaceans (e.g., Cabezas et al., 2008, 2009 for Munididae). The mitochondrial partial COI and 16S genes were used to infer phylogenetic

relationships between evolutionary significant units (ESUs sensu Moritz, 1994). Additionally, the nuclear Histone 3 (H3) gene marker was employed to assess whether hybridization may have occurred among the lineages, due to biparental inheritance and eventual crossing-over during meiosis of the nuclear markers, and to verify if a biological species concept can be applied.

Our objectives are to: (a) investigate the extend of hidden morphological and genetic diversity; (b) assess congruence between morphological differentiation and molecular phylogenies; and (c) elucidate phylogeographic relationships among ESUs within this species complex against contrasting biogeographic hypotheses. *U. naso* and two previously unrecognised new species are described. New species epithets reflect the name of the original species, *naso* meaning nose.

2. Materials and methods

2.1. Specimen collection and identification

Ethanol-preserved specimens were collected during a survey in 2007 of the macrofauna of the continental slope of northern Western Australia (a northern extension of the sampling in southern WA reported by Poore et al., 2008) and now housed in Museum Victoria (NMV). Additional ethanol-preserved specimens were

Table 1

Specimens analyzed in this study. #, specimen catalogue number for tissue. Details of station locations are given with material examined in the taxonomic section. Catalogue numbers 56 and 145 were supplied by C.-W. Lin, NTOU.

#	Haplotype	Clade	Voucher location	Voucher registration	Sampling site	Depth (m)	Collection year	GenBank Acc numbers COI/16S/H3
Uroptychus naso Van Dam, 1933								
175	–	–	ZMA	De.101.667	Indonesia, Kei Is, Siboga stn 251	–	–	–/–/JF715103
176	–	–	ZMA	De.101.692	Indonesia, Kei Is, Siboga stn 153	–	–	–
177	–	–	NTOU		Taiwan, Nang fang-Ao	–	1995	–/JF715120/JF715099
11	1	I	NTOU		Taiwan, stn CP115	381–440	2001	JF715132/–/–
180	1	I	NTOU		Taiwan, Su-Ao	–	1998	JF715138/JF715121/JF715095
56	11	I	NTOU		Taiwan, stn CP216	209–280	2003	JF715133/JF715124/JF715097
145	12	I	NTOU		Taiwan	–	–	JF715134/–/–
185	13	II	NTOU		Philippines, stn CP2343	309–356	2001	JF715140/JF715126/JF715101
186	14	II	NTOU		Philippines, stn CP2343	309–356	2001	JF715141/JF715127/JF715102
187	15	II	NTOU		Philippines, stn CP2343	309–356	2001	JF715139/JF715123/JF715098
29A	2	III	NMV	J60839	Australia, WA, stn 095	206–202	2007	JF715142/JF715129/JF715094
219	2	III	NMV	J60838	Australia, WA, stn 112	202–191	2007	JF715143/JF715128/JF715092
29B	3	III	NMV	J56118	Australia, WA, stn 095	206–202	2007	JF715137/JF715130/JF715093
42	9	III	NMV	J56128	Australia, WA, stn 099	211–205	2007	JF715135/JF715119/JF715090
45	10	III	NMV	J57259	Australia, WA, stn 098	206–187	2007	JF715136/JF715118/JF715091
179	–	–	NTOU		Taiwan, Dasi	–	1991	–/JF715125/–
181	–	–	NTOU		Taiwan, stn CP115	381–440	2001	–
182	–	–	NTOU		Taiwan, stn CP114	128–250	2001	–/JF715122/JF715096
183	–	–	NTOU		Taiwan, stn CP114	128–250	2001	–/–/JF715100
222	–	–	ZMUC	CRU-11333	Indonesia, Kei Is	245	1922	–
223	–	–	ZMUC	CRU-11335	Indonesia, Kei Is	268	1922	–/–/JF715104
224	–	–	ZMUC	CRU-20206	Indonesia, Kei Is	245	1922	–
225	–	–	ZMUC	CRU-20207	Indonesia, Kei Is	270	1922	–
Uroptychus cyrano new species								
31A	7	IV	NMV	J57256	Australia, WA, stn 6	210–205	2007	JF715144/JF715109/JF715082
31B	5	IV	NMV	J57256	Australia, WA, stn 6	210–205	2007	JF715146/JF715116/JF715084
213	5	IV	NMV	J57256	Australia, WA, stn 6	210–205	2007	JF715152/JF715110/JF715085
214	16	IV	NMV	J57256	Australia, WA, stn 6	210–205	2007	JF715147/JF715114/JF715078
215	17	IV	NMV	J57256	Australia, WA, stn 6	210–205	2007	JF715148/JF715111/JF715079
32	8	V	NMV	J57262	Australia, WA, stn 142	210–203	2007	JF715155/JF715117/JF715083
30A	5	IV	NMV	J57263	Australia, WA, stn 112	202–191	2007	JF715145/JF715106/JF715088
30B	6	V	NMV	J57263	Australia, WA, stn 112	202–191	2007	JF715153/JF715107/JF715086
217	8	V	NMV	J57263	Australia, WA, stn 112	202–191	2007	JF715156/JF715113/JF715081
218	18	IV	NMV	J57263	Australia, WA, stn 112	202–191	2007	JF715151/JF715115/JF715087
216	16	IV	NMV	J60841	Australia, WA, stn 112	206–202	2007	JF715150/JF715112/JF715080
29C	4	IV	NMV	J60841	Australia, WA, stn 095	206–202	2007	JF715149/JF715108/JF715089
Uroptychus pinocchio new species								
178	–	–	NTOU	–	Taiwan, Aodi	–	2000	–/ JF715131/–
226	–	–	ZMUC	CRU-20208	Japan, Kyushu	189	1898	–/–/JF715105

borrowed from: the National Taiwan Ocean University (NTOU) collected off Taiwan and the Philippines: the Zoological Museum, University of Copenhagen (ZMUC), collected from the Kei Islands, Indonesia, and Japan; the Muséum nationale d'Histoire naturelle, Paris (MNHN) from Indonesia and the Philippines; and type material, Kei Islands, Indonesia, was borrowed from the Zoological Museum, Amsterdam (ZMA). It is probable that some of the museum material was preserved in formalin (see Table 1 for details). These localities cover the published distribution of the species with the addition of WA. Our material totalled 72 specimens. Only selected specimens have been included in the molecular analysis.

2.2. Morphological treatment

The delineation of new species was based first on targeting genetically distinct ESUs. ESUs are here intended as highly statistically supported assemblages of sequences containing low intra-clade genetic divergence. Only the COI marker was deployed for initial identification of highly supported clades. The ESUs correlated with geographical distribution, common gross morphology and color patterns of populations (as represented by our limited samples) were examined in detail. In this way ESUs respect the phylogenetic species concept and are characterized by distinct evolutionary trajectories although the possibility of interbreeding is not excluded. New taxa are described by modifying a DELTA database (Dallwitz et al., 1999) volunteered by Kareen Schnabel (Schnabel, 2009) and incorporating characters from recent descriptions of new species of *Uroptychus* (Baba and Lin, 2008). By the traditional standards of chirostylid taxonomy the differences between taxa described here might be considered slight. Dimensions are total carapace length including rostrum (tl.), widest carapace width including branchial spines (cw.) and width between antennal spines (aw.). Total lengths and relative length of articles of the cheliped were measured from photographs and are means from several specimens. The relative lengths of articles of other pereopods were measured along the extensor margin from illustrations.

2.3. DNA extraction, PCR amplification and sequencing

Total DNA was extracted from 50–100 mg ethanol- or formalin-preserved abdominal tissue or pereopod of the target specimen following the salt-based extraction procedure described by Aljanabi and Martinez (1997) with minor modifications. We are not sure whether specimens from ZMA and ZMUC have been initially preserved in formalin. Yet, due to the limited amount of tissue, DNA from these specimens could not be extracted with an extraction protocol suitable for formalin-fixed tissues. These specimens were therefore washed (2×30 min) in buffer containing 10 mM PBS, 27 mM KCl and 137 mM NaCl prior DNA extraction as aforementioned; PCR reactions were performed in combinations of variable concentrations of oligos, MgCl₂, Bovine Serum Albumin, relaxed annealing temperatures and different TAQ enzymes. Quantity and quality of DNA were examined by means of 1% agarose TAE buffer gel electrophoresis against known standards.

Partial COI and 16S sequences were PCR-amplified using the primer pair LCO1490-HCO2198 described by Folmer et al. (1994) and the primer pair 16Sarl–16Sbrh described by Palumbi and Benzie (1991) respectively. The H3 Histone gene was PCR-amplified using the primer pair H3F–H3R published by Colgan et al. (1998). Standard PCR reactions were performed in 30 μl of medium containing approximately 10 ng DNA, 1.5 mM MgCl₂, 0.2 mM dNTPs, 1 μM of forward and reverse primers each, 1× PCR reaction buffer and 1.25 units of *iTaq* DNA polymerase (Scientifix). The amplification cycle for the partial COI marker included an initial denaturation at 94 °C for 4 min followed by 35

cycles of 94 °C 1 min, 50 °C 1 min and 72 °C 1.5 min followed by a final extension cycle at 72 °C for 7 min. The partial 16S gene was amplified under the same conditions except for the lower annealing temperature (45 °C). The Histone 3 was amplified under the same reaction conditions and 94 °C for 3 min followed by 30 cycles of 94 °C 30 s, 55 °C 30 s, and 72 °C 40 s followed by a final extension cycle at 72 °C for 7 min. Quantity and length of the PCR-products were examined by 1% gel electrophoresis as described above. Multiple amplification products were never observed. PCR reactions were sent to Macrogen Inc. (Korea, www.macrogen.com) for purification and direct sequencing on both directions.

Standard protocols for DNA extraction were used on museum specimens of uncertain preservation history (given the small amount of tissue available) including the type specimens.

2.4. Sequence alignments and phylogenetic analysis

Nucleotide sequences were assembled using the computer software Sequencher 4.9 (Gene Codes). Partial COI and Histone 3 sequences were aligned manually in Bioedit v7.0.9 (Hall, 1999). Because many regions of the partial 16S gene are extremely divergent and may produce unreliable alignments, sequences were either aligned in Bioedit using the ClustalW algorithm (Thompson et al., 1994) with several gap openings and extension penalties or in MUSCLE (http://www.ebi.ac.uk/Tools/muscle/index.html). The latter is known to achieve the highest accuracy scores so far reported (Edgar, 2004). Finally, 16S alignments were refined by eye.

Phylogenetic information was assessed by calculating g_1 statistics as a measure of the skewness of distribution of three-lengths among 10000 random parsimony trees (Hillis and Huelsenbeck, 1992) 1992 in PAUP∗. The significance of the g_1 value was compared with critical values ($p = 0.01$) for four state characters given the number of distinct sequences and the number of parsimony informative sites. Hierarchical Likelihood Ratio Tests (hLRTs) were computed in Modeltest Version 3.7 (Posada and Crandall, 1998) to identify the best-fitting parameters (substitution model, gamma distribution, proportion of invariable sites, transition–transversion ratio) for Bayesian inference (BI) and maximum likelihood (ML) analyses given the alignment. We used the GTR substitution model when the Modeltest output could not be implemented in MrBayes. In these cases model parameters were treated as unknown variables with uniform default priors and were estimated as part of the analysis.

Outgroup comparisons of the concatenated mitochondrial dataset were performed against partial COI and 16S sequences of *Pagurus pollicaris* and *P. bernhardus* (Paguridae). Maximum parsimony (MP) and ML phylogenies were conducted in PAUP∗ 4.0b10 version for Windows (Swofford, 2002). Bayesian inference for posterior probability estimates of the nodes coupled with Markov chain Monte Carlo (MCMC) algorithm was implemented in MrBayes v3.1.2 (Huelsenbeck and Ronquist, 2001). MP trees were inferred using the heuristic search option, 500 random sequence additions and tree bisection–reconnection (TBR) branch swapping. Characters were unweighted and treated as unordered and gaps were treated as missing data. BI and ML computations were constrained with the best fitting model of evolution identified by Modeltest. ML heuristic searches were run in PAUP∗ under ten random additions and TBR branch swapping. BI was conducted for 5000,000 generations of two parallel runs of four chains each, starting from a random tree and sampling every 1000th generation. The convergence of the parameter estimates was graphically confirmed by plotting values of likelihood against the generation time in Tracer v1.5 (Rambaut and Drummond, 2007). Bootstrap support for individual clades in MP an ML was calculated on 1000 replicates using the same methods, options and constraints as used in the tree-inferences but with all identical sequences removed (Felsenstein,

1985). Genealogical relationships among sequences within cryptic species were calculated using the Median Joining algorithm ($\varepsilon = 0$, equally weighted characters) implemented in the software Network v4.5.1.6 (http://www.fluxus-technology.com). The method identifies groups of closely related haplotypes and uses "median vectors" to connect sequences into a tree or network. Median vectors can be interpreted biologically as extinct individuals or haplotypes that have not been sampled yet (Bandelt et al., 1999).

Table 2
Sequence and alignment statistics. *l*, alignment length; *n*, number of new sequences; *h*, number of haplotypes; *c*, number of clades; g_1, phylogenetic informativeness of the data; *m*, evolutionary model selected by Modeltest; *v*, variable, parsimony uninformative sites; *p*, parsimony informative sites.

	l	*n*	*h*	*c*	g_1	*m*	*v*	*p*
COI	669	24	18	4	−0.34	HKY + I	40	165
16S	450	26	15	3	−0.77	K81uf + G	61	77
H3	346	28	4	3	−0.33	–	4	4
COI-16S	1122	–	–	3	−0.33	–	104	234
COI-16S-H3	1472	–	–	4	−0.35	–	104	238

2.5. Divergence times estimates

The concatenated COI-16S-H3 alignment was engaged in BEAST v.1.5.4 (Drummond and Rambaut, 2007) to approximate divergence times among cryptic species using an uncorrelated lognormal relaxed clock method which accounts for clade-specific rate heterogeneity (Drummond et al., 2006) under a HKY + I + G model and a speciation Yule process as tree prior. Specimen 178, belonging to *Uroptychus pinocchio,* was excluded from the computation due to missing data from two out of three markers. Results relate only to the other two species of *Uroptychus*. The H3 Histone gene was included in the analysis in order to take advantage of the conservative nature of this marker, capable of detecting deep cladogenesis events within the *U. naso* complex (clade ((I, II) III) from clades (IV, V). Three fossil records were identified as calibration points on the basis of the earliest representative at a particular taxonomical level for that node. These are: *Munida primaeva* Segerberg, 1900 (Galatheidae) of Danian age, 61.7–65.5 MYA (Jakobsen and Collins, 1997); *Haumuriaegla glaessneri* (Aeglidae) of Haumurian age, 66–80 MYA (Feldmann, 1984) and *Protaegla miniscula* (Aeglidae) of Albian age, 99.6–112 MYA (Feldmann et al., 1998). Another, *Pristinaspina gelasina* Schweitzer and Feldmann, 2000
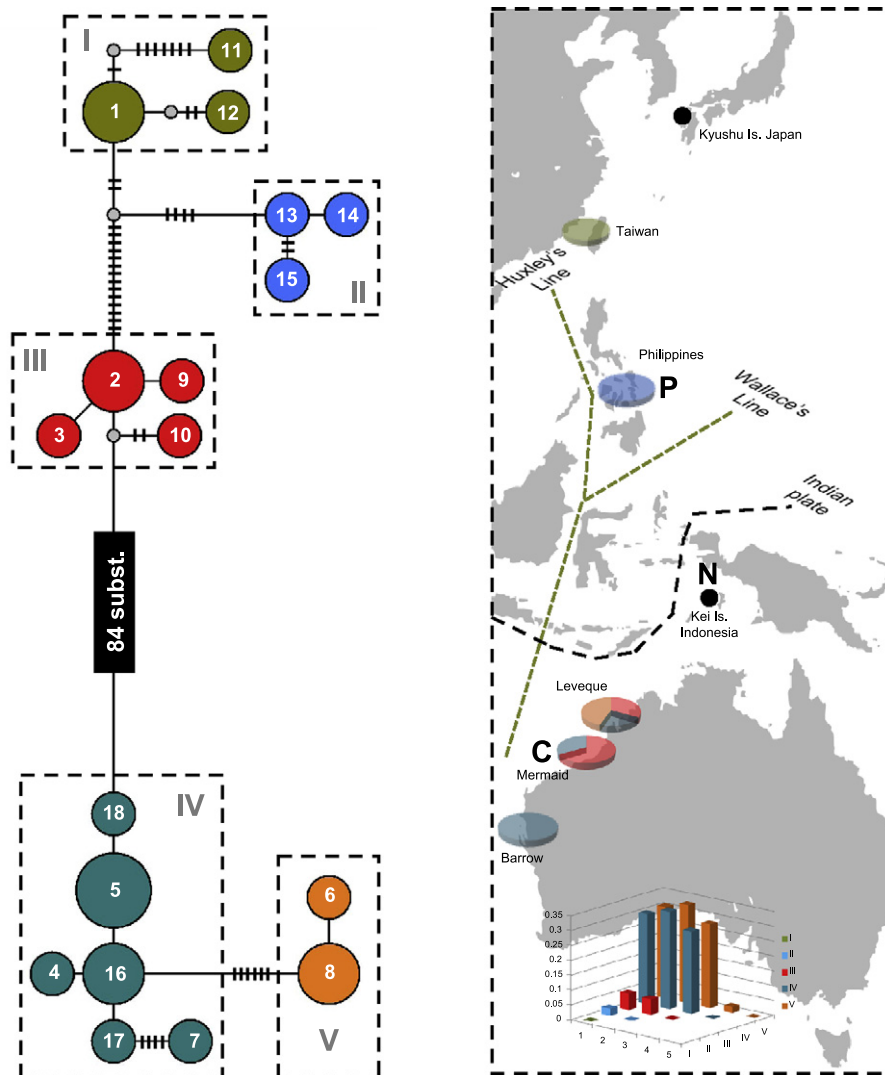

Fig. 1. Median-joining network reconstruction based on 555 bps of the mitochondrial COI marker. Circles represent haplotypes; numbers in circles, haplotype id; circle size is proportional to the frequency of that haplotype; bars across lines connecting haplotypes indicate base changes. C, N and P represent the type localities of the three species, *U. cyrano, U. naso* and *U. pinocchio*; histogram, pairwise K2P distances between mitochondrial clades.

(Cenomanian to Maastrichtian age, 65.5–99.6 MYA), once considered the first chirostylid in the fossil record, was not employed in the computations given its recently recognised shared morphological characters with Kiwaidae (Ahyong et al., in press; Schnabel and Ahyong, 2010). Posterior distributions of divergence time approximation with 95% intervals of credibility were obtained following a MCMC computation of 10,000,000 generations, sampling every 1000th generation and an initial burnin of 10,000 generations. Convergence of the run and exploration of the results were done in Tracer v1.5 by plotting values of likelihood against the generation time (Rambaut and Drummond, 2007).

3. Results

3.1. Phylogenetic analysis

A total of 24, 26 and 28 new sequences was obtained from the COI, 16S and H3 DNA regions respectively (see Table 2 for sequences, alignment length, model selection and summary statistics). Only H3 sequences were obtained from the specimens from ZMA and ZMUC. Sequence analysis for these specimens was repeated several times to ensure reliability of this result. Length distribution of 10,000 random trees computed for single marker and concatenated alignments were considerably left-skewed indicating significant levels of phylogenetic structure in the datasets (Table 2). Four different datasets of putative U. naso sequences were analyzed for phylogenetic and phylogeographic inference: (1) a trimmed 555 bp alignment of COI sequences for median joining network reconstructions; (2) a concatenated COI-16S alignment; (3) only the H3 alignment; (4) a concatenated COI-16S-H3 alignment with specimens 178, 179 excluded due to missing data from COI and H3 genes. Model-constrained BI, ML and MP analyses (not shown), inferred from the COI marker, revealed five highly differentiated ESUs (clades I–V) characterized by strong bootstrap support and low intra-clade sequence divergence (see genealogical network reconstruction in Fig. 1 and Table 3a for distances). COI ESUs were further structured into two major sister clades diverging $p = 15.7\%$ from one another: clade ((I, II) III) and clade (IV, V). Topologies obtained from model-constrained BI, ML and MP analyses of the partial 16S gene (data not shown; see Table 3b for distances) and the concatenated COI-16S dataset (Fig. 2a) were congruent. Yet, in both cases, ESU II was less supported thus forming a unique cluster within clade I. ESU III was strongly supported by several substitutions in COI and 16S gene regions. ESU IV was statistically weaker alone but formed a single statistically robust cluster with ESU V. The nuclear H3 was less informative, yet able

Table 3
K2P distance calculations for the COI and 16S markers. m, K2P mean diversity within-ESUs; d, coefficient of differentiation estimated as the proportion of inter-ESU diversity.

COI	U. naso			U. cyrano		m	d
	I	II	III	IV	V		
I	–					0.0161	0.961
II	0.024	–				0.0036	
III	0.056	0.052	–			0.0065	
IV	0.304	0.328	0.277	–		0.0052	
V	0.308	0.331	0.283	0.02	–	0.0015	

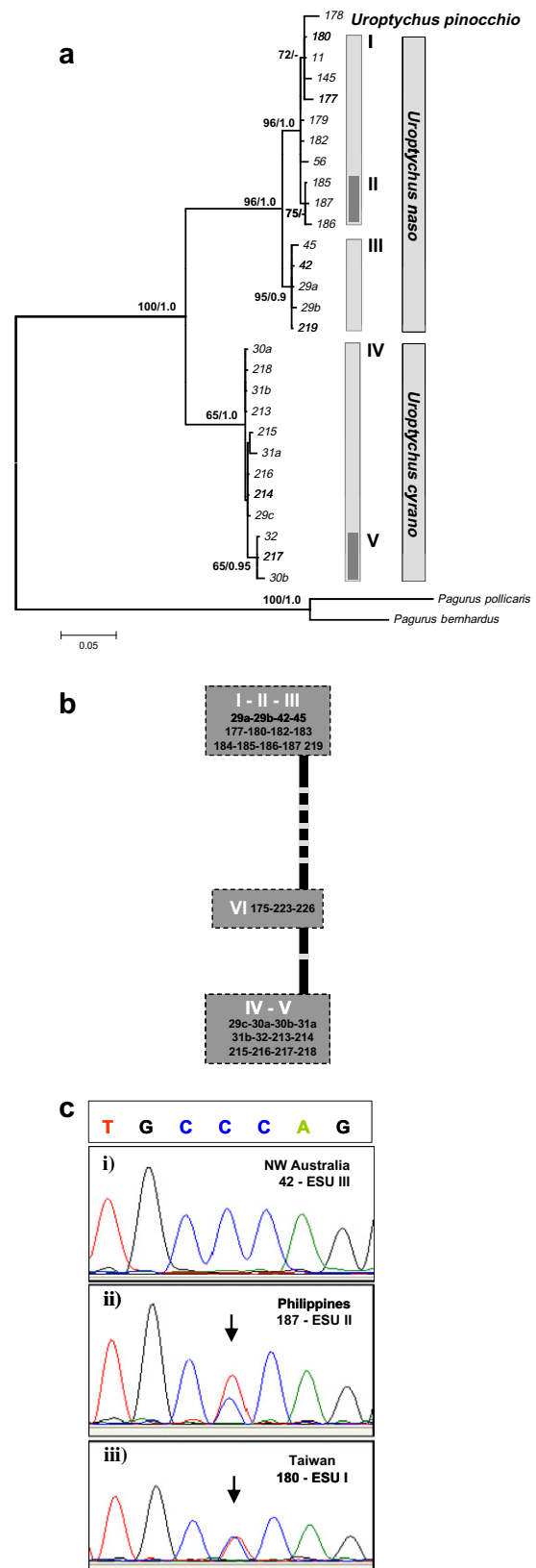| 16S	I + II	III	IV + V	m	d
I + II	–			0.00642	0.852
III	0.01342	–		0.00182	
IV + V	0.04214	0.03818	–	0.00247	

Fig. 2. (a) Maximum likelihood phylogeny based on bi-partitioned concatenated mitochondrial regions; numbers on nodes indicate ML bootstrap support and Bayesian posterior probabilities respectively; letters on clades indicate ESUs identified by the COI marker, (b) median network reconstruction obtained from the H3 Histone; clade and specimen numbers are reported in each box; gray lines connecting circles indicate base changes and (c) selected sites on H3 Histone alignment showing degenerated positions.

to clearly resolve the assemblage of ESUs I–III from the sister cluster IV + V by five synapomorphies and cluster of IV + V from a new ESU, VI, by one (Fig. 2b). No genetic variability was encountered at the within-ESU level indicating the low evolutionary speed of the H3 marker. Additionally, all specimens of mitochondrial ESUs I and II from Taiwan and Philippines were characterized by two unresolved positions at the nuclear marker, when compared to ESU III, scored following the degenerated genetic code (Fig. 2c). ESU VI included only museum material from Kei Islands and Japan (2 and 1 sequences respectively) that we assume were formalin-fixed. Of the three markers, only the H3 gene was successfully sequenced, mainly due to the difficulties in obtaining suitable quality of DNA for PCR amplification. Given its lower resolution power and in the absence of support from at least one mitochondrial gene region, we consider the sole H3 gene taxonomically unreliable. Clade VI had no morphological support.

3.2. Species differentiation

The re-examination of Western Australian specimens belonging to clades III and IV + V (Fig. 1) revealed two morphologically distinct species. Following comparison with type material we have concluded that clades I–III and other material available to us

belong to *U. naso*. Clade IV + V represents a second species, a Western Australian endemic, described as new below. Smaller differences, between clades I, II and III, and between IV and V, were not detected in the morphology and are discussed below. One exceptional sequence from a specimen from Aodi, Taiwan (sequence 178) fell within the *U. naso* clade I but was morphologically quite distinctive. Baba et al. (2009a) remarked on this specimen and its color photo illustrates a color pattern different from others from Taiwan. This specimen and others from the NW Pacific belong to a second new species that can be differentiated morphologically but for which we have no reliable molecular data.

3.3. Divergence times estimates

Estimates from a log-normal uncorrelated relaxed molecular clock using two independent calibration fossils, suggested two intervals of major cladogenesis events, responsible for speciation within the *U. naso* species complex. A first event took place in late Cretaceous, approximately 80 MYA (95% credibility interval: 66.16–98.03 MYA), separating the new species, *U. cyrano* (mitochondrial clades IV and V) from *U. naso* (mitochondrial clades I–II–III; 95% credibility interval: 30.06–77.01 MYA). Apparently, populations of *U. naso* colonized Western Australia, Indonesia,
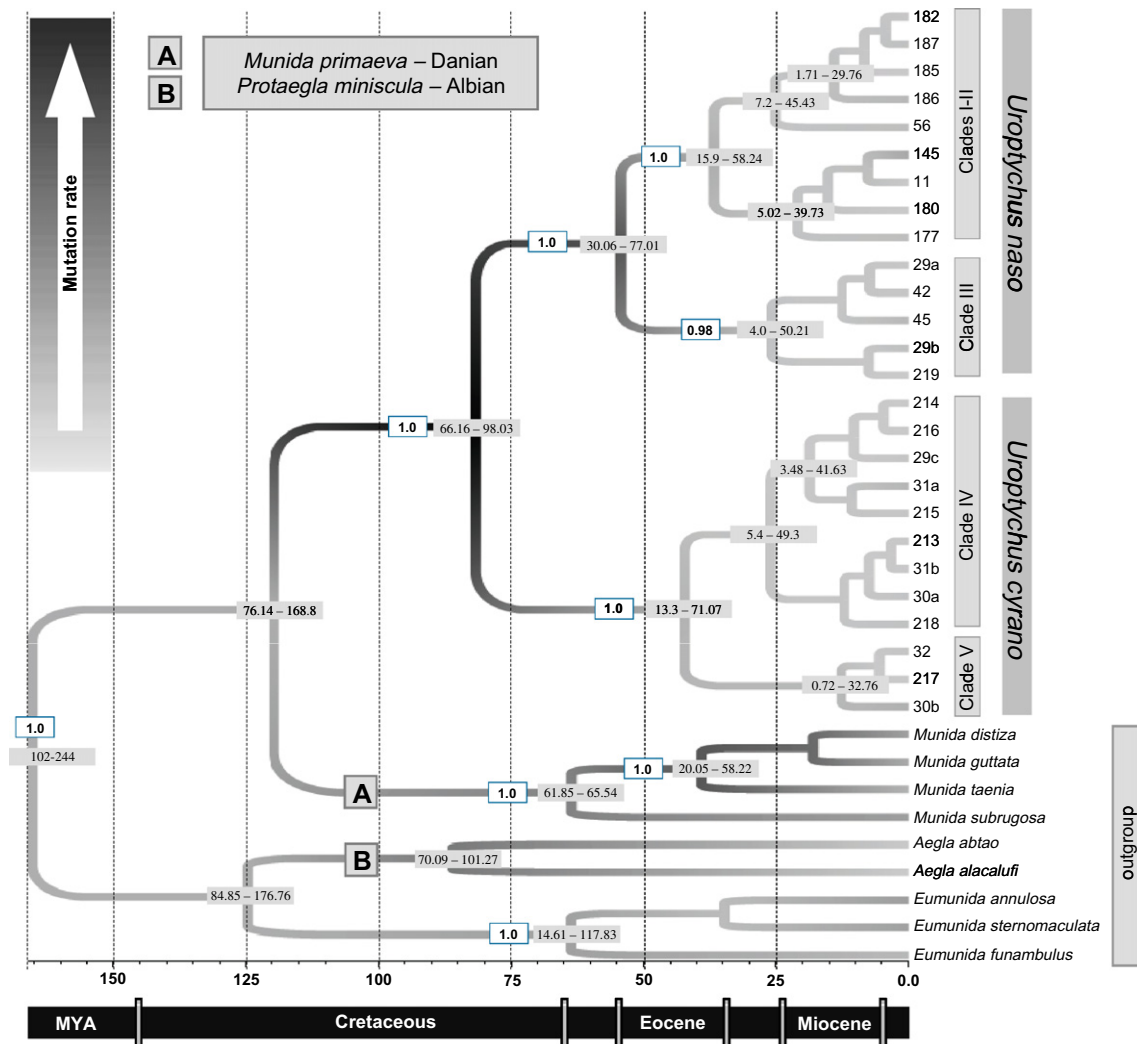

Fig. 3. Divergence time estimates of *Uroptychus* spp. with 95% credibility intervals in major nodes (numbers in gray boxes) based on the concatenated dataset (COI-16S-H3). Specimens 178 and 179 have been excluded from the computation due to missing data. Calibration fossils and nodes are reported as A and B. Color gradient throughout the topology indicates changes in mutation rate. A time scale in MY before present and a geological time scale is given below.

Philippines, Taiwan and Japan in late Oligocene and diverged into genetically distinct populations during Miocene. We consider *Uroptychus cyrano* (mitochondrial clades IV and V) to be a Tethys relict, in this study endemic to Western Australia, although the presence of this species in Indonesia cannot be excluded. Independently of the directionality of dispersal, genetically distinct populations of *U. naso* are here considered as the result of multiple colonization events followed by geographical isolation that may have commenced in early Miocene.

4. Taxonomy

4.1. Uroptychus. naso Van Dam, 1933

See Figs. 4a, 5a, 6 and 7.

4.1.1. Synonymy
Uroptychus naso Van Dam (1933: p. 23, Figs. 35–37; Van Dam (1939: 402, one specimen only, see *U. pinocchio*; Van Dam (1940:

p. 97; Baba (1969: p. 42–45 (part), Fig. 2a; Baba (1988: p. 39; Wu et al. (1998 (1997): p. 81, Fig. 5, color Fig. 12B; Baba (2005: p. 49, 228; Baba et al., (2008Baba et al., 2008: p. 37, color fig. 1F; Wang (2008: p. 750; Baba et al. (2009: p. 47–48 (part), Figs. 38 (color), 40.

4.1.2. Material examined
Types. Indonesia, Kei Is, Kur I. and Taam I., 304 m (*Siboga* stn 253), ZMA De. 101.692 (syntypes: male, 16.9 mm; male, 13.0 mm); 204 m (*Siboga* stn 251), ZMA De. 101.667 (syntypes: male, 18.8 mm, female fragmented).

Other material. Japan. E of southern Kyushu, 32°19′N, 128°12′E, 153–363 m, 1 September 1932, Store Nordiske Telegraf Comp. (det. A.J. Van Dam), ZMUC CRU-20227 (male, 16.0 mm).

Taiwan. Locality listed by place name are fishing ports where by-catch was sampled. Nanfang-Ao, 9 Nov 1995, NTOU A00976 (ovigerous female, 15.2 mm). Su-Ao, 14 May 1998, NTOU A00978 (ovigerous female, 13.9 mm). Dasi, 5 June 1991, NTOU A00979 (male, 15.4 mm); 19 October 1995, NTOU (male, 15.8 mm). Stn CP114, 24°51.03′N, 121°58.30′E, 128–250 m, 21 November 2001,
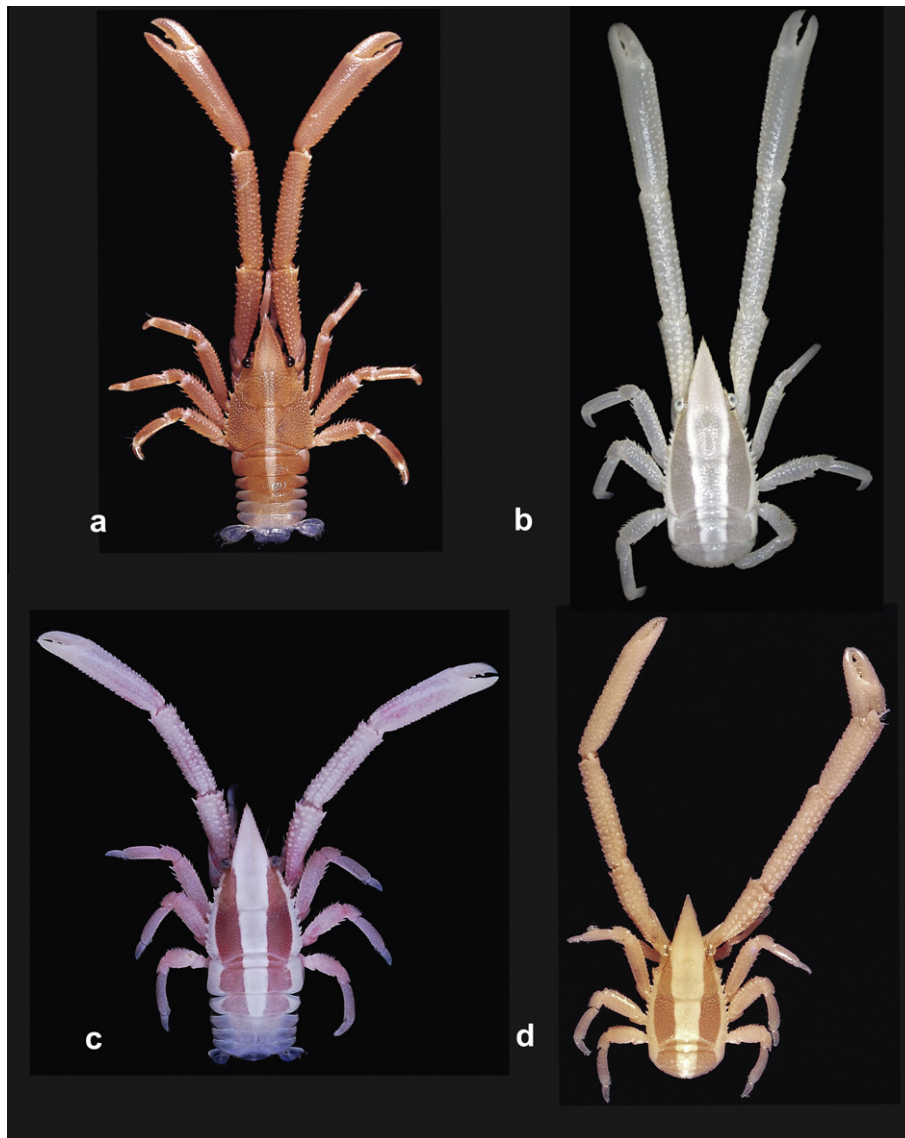

Fig. 4. (a) *Uroptychus naso* Van Dam, 1933, Taiwan, NTOU stn CP115. (b) *Uroptychus cyrano* new species, Western Australia, stn SS05/2007 006, NMV J57256. (c) *Uroptychus pinocchio* new species, Philippines, 2008 LUMINWAN stn CP2865 (specimen not seen). (d) *Uroptychus pinocchio* new species, Taiwan, Aodi, NTOU. Photos a, c and d by T.-Y. Chan; b by K. Gowlett-Holmes. Not to same scale.
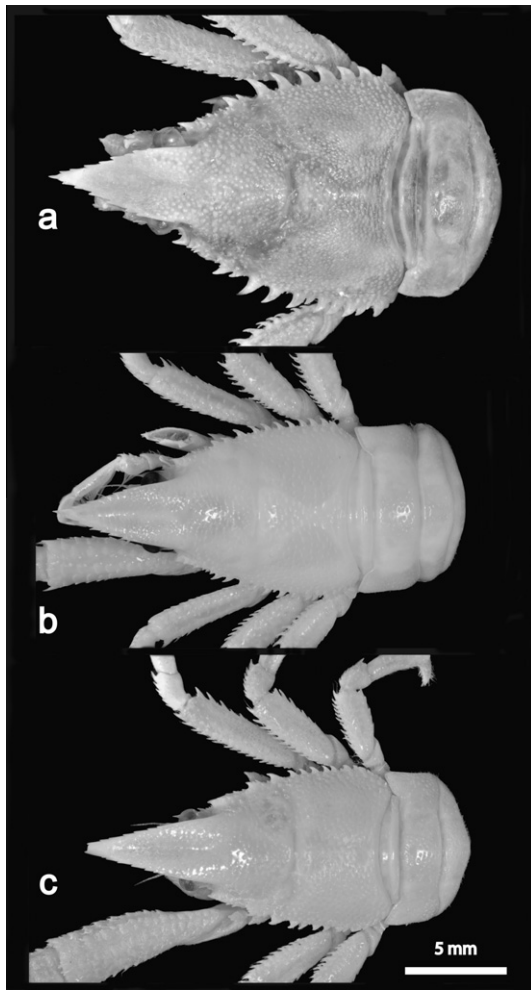
Fig. 5. (a) *Uroptychus naso* Van Dam (1933), syntype, *Siboga* stn 253, ZMA. (b) *Uroptychus cyrano* new species, Western Australia, stn SS05/2007 142, NMV J57262. (c) *Uroptychus pinocchio* new species, Philippines, MUSORSTOM stn 61, MNHN Ga6230.

NTOU A00981 (ovigerous female, 14.9 mm; male, 10.2 mm). Stn CP115, 24°53.87′N, 122°02.05′E, 381–440 m, 21 May 2001, NTOU A00982 (male, 15.2 mm). Stn CP216, 24°34.71′N, 122°04.02′E, 209–280 m, 27 August 2003, NTOU A00983 (male, ~15 mm).

Philippines. Panglao, 09°26.6′N, 123°51.3′E, 309–356 m, 23 May 2005 (stn CP2343), NTOU A00984 (female with small *Sacculina* externa, 17.5 mm; female, 15.2 mm; male, 15.2 mm, 17.9; male with paired sacculinid externae, 17.9 mm). 14°00.5′N, 120°16.5′E, 189–192 m, 1980 (MUSORSTOM 2 stn CP19), MNHN Ga 6233 (1 ovigerous female, 18.1 mm), MNHN Ga 6231 (male, 19.1 mm). 14°0′N, 120°10′E, 170–174 m, (MUSORSTOM 2 stn CP54), MNHN Ga 6236 (male, 17.7 mm). 13°59′N, 120°18.5′E, 186–187 m, 1976 (MUSORSTOM stn 35), MNHN Ga 6228 (male, 19.1 mm). 14°1′N, 120°17′E, 215–216 m, 1980 (MUSORSTOM 2 stn CP53), MNHN Ga 6235 (three males, max. 15.4 mm). 14°1.7′N, 120°16′ E, 183–185 m, 1976 (MUSORSTOM stn 3), MNHN Ga 6227 (1 ovigerous female).

Indonesia. Kei Is, 5°48.5′S, 132°14′E, 270 m, sand, 1 May 1922 (Th. Mortensen stn 45), ZMUC CRU-20207 (ovigerous female, 17.9 mm); 5°37.16′S, 132°26′E, 245 m, sand, 3 May 1922 (Th. Mortensen stn 49), ZMUC CRU-20206 (male, 18.0 mm), ZMUC CRU-11333 (male, 13.4 mm); ?locality, 268 m, 30 April 1922 (Th. Mortensen stn 44), ZMUC CRU-11335 (female with *Sacculina* externa, 17.0 mm). Kei Is, 5°17′N, 132°50′E, 315–349 m, 24 October

1991 (KARUBAR stn CP16), MNHN Ga 4204 (male, 13.0 mm). Tanimbar I., 225–223 m, (KARUBAR stn CP86), MNHN Ga 4196 (four females, three males, max. 15.7 mm). 296–299 m, (KARUBAR stn CP05), MNHN Ga 4171 (male, 13.8 mm). 9°32′N 131°2′E, 219–217 m, 4 November 1991 (KARUBAR stn CP82), MNHN Ga 4162 (three females, two males, max. 12.5 mm).

Australia. WA, near Mermaid Reef, 17°26.1′S, 120°26.4′E, 206–202 m, 20 Jun 2007 (stn SS05/2007 095), NMV J60847 (male, 16.5 mm); NMV J56118 (ovigerous female, 14.0 mm). Off Point Leveque, 15°0.8′S, 121°43.1′E, 205–211 m, 25 Jun 2007 (stn SS05/2007 099), NMV J56128 (two males, 9.4, 4.5 mm). 14°59.4′S, 121°39.1′E, 206–187 m, 25 June 2007 (stn SS05/2007 098), NMV J57259 (male, 11.0 mm). 14°58.1′S, 121°40.6′E, 203–210 m, 2 July 2007 (stn SS05/2007 142), NMV J60837 (male, 10.7 mm). 14°58.8′S, 121°40.2′E, 202–191 m, 28 June 2007 (stn SS05/2007 112), NMV J60838 (two males, 7.5, 4.7 mm).

4.1.3. Description

Carapace moderately convex from side to side, total length (tl.) 1.43 times greatest width (cw.) in males, 1.36 in females (range, 1.28–1.52); distance between antennal spines (aw.) 0.49 times greatest width (cw.). Rostrum narrowly triangular, with shallow groove in dorsal midline, with rounded ventral ridge, depressed anteriorly, length 0.4 times total length; dorsal surface with tubercles except in midline; lateral margin with 7–9 blunt teeth along distal two-thirds. Cervical groove at about midlength of carapace, deep medially (indistinct cervical groove and groove between anterior and posterior branchial regions laterally). Carapace covered with conical tubercles, spine-like laterally, strongest on anterior branchial region, with scattered setae; frontal margin transverse (with small spine at midpoint); antennal spine sharp, well produced; anterolateral margin irregularly covered with short spines; branchial margin strongly convex; anterior branchial margin with strong spine, more or less unequally bifid, covered with spinules; posterior branchial margin with 6–7 strong spines, decreasing in length and becoming broader and more closely spaced posteriorly, obscurely dentate over most posterior fifth. Pterygostomial flap irregularly covered with small tubercles, anterior margin with prominent upturned spine (and smaller denticles).

Sternal plastron (sternites 3–7) one times as long as wide, widening posteriorly; excavated sternum rounded anteriorly, with sharp midventral ridge; sternite three slightly depressed relative to sternite 4, anterior margin excavate, with U-shaped median sinus (sinus obscurely dentate), lateral margin rounded anterolaterally, irregularly denticulate laterally, surface smooth; sternite four anterior margin 0.64 times as wide as posterior margin, anterolaterally angled, surface tuberculate.

Abdominal somites smooth (except for transverse granular ridge on somite 1); tergites rounded anteriorly and posteriorly.

Telson 0.4 times as long in midline as greatest width; anterior section 0.5 times as long as midline length; anterolateral lobes projecting beyond posterolateral lobes, broadly rounded to subtly truncate, setose; posterior margin shallowly excavate, evenly setose.

Eyestalk 0.33 times length of rostrum; cornea globular, pigmented.

Antennule article 1 with laterodistal triangular scale; article 3, 2.4 times as long as wide. Antenna articles 3–5 with distomesial spines on all articles; article 5, two times as long as article 4; antennal scale reaching to end of lateral margin of article 5, 3.7 times as long as wide, lateral margin with small spine or without spines.

Maxilliped three merus with 1 distolateral spines, three lateral marginal spines; carpus with seven spines along extensor margin.
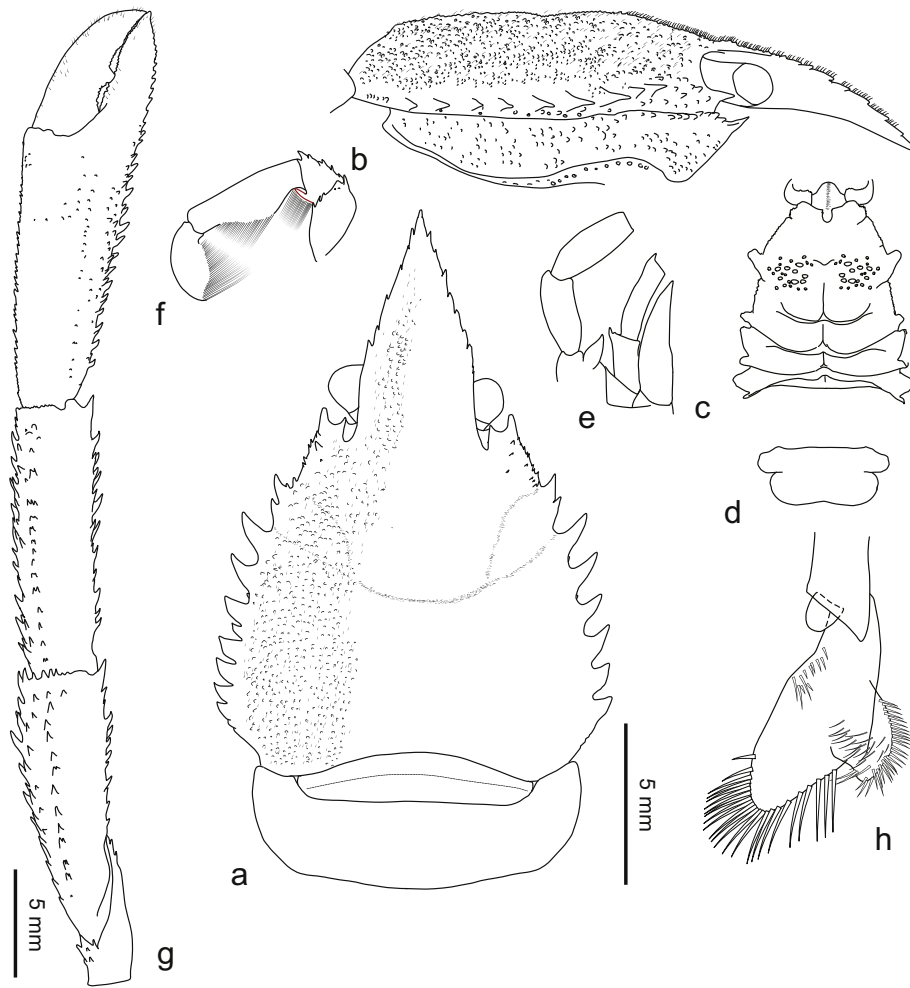
Fig. 6. *Uroptychus naso* Van Dam, 1933. (a and b) Carapace in dorsal and lateral views. (c) Sternal plastron. (d) Telson. (e) Left antennule and antenna, ventral view. (f) Left maxilliped 3, lateral view. (g) Right pereopod 1, upper face in situ. (h) Right pleopod 1, lateral view. (a–f) From syntype, ZMA, *Siboga* stn 253. (h) From male, NMV J60847. Pereopod 1 drawn at 2/3 scale of carapace, sternum and telson.

Pereopod 1 of adult male 2.9 times as long as carapace (max.), female 2.6 times as long as carapace (max.), with scattered setae, especially on fingers; ischium with prominent complex thorn-like projection on upper margin; merus with oblique spines, more or less in three rows, along extensor margin, with row of oblique spines in row on upper face, and with numerous oblique spines, more or less in two rows, along flexor margin; carpus 1.1 times as long as ischium, with numerous oblique spines, more or less in row, along extensor margin, with row of oblique spines, several duplicated, on upper face, and with numerous oblique spines, more or less in 3 rows, along flexor margin; propodus 1.4 times as long as carpus, width at base of fingers 1.9 times distal width of carpus in adult, with scattered prickles over extensor margin and upper surface and with about 23 spines in two uneven rows along flexor margin, cutting edge of fixed finger denticulate, evenly convex; dactylus 0.38 times as long as total length of propodus, upper margin smooth, setose, with one tooth on cutting edge, cutting edge with prominent blunt tooth about one-third along, curved and denticulate beyond.

Pereopods 2–4 diminishing in relative length anterior to posterior (85%), with strongly spinose ischium–carpus and with scattered setae. Pereopod 2 ischium with two spines distally on extensor margin; merus 0.44 times as long as total length of carapace, 3.8 times as long as broad, with row of c. 13 oblique spines along extensor margin, row of spinules laterally and with three prominent spines distally on flexor margin, smaller ones proximally; car-pus with seven sharp spines along extensor margin; propodus 0.55 times as long as merus, 3.2 times as long as wide, with row of nine robust setae along flexor margin plus pair distally, with clusters of long setae on extensor margin and with short rows of setae on me-sial and lateral faces; dactylus 0.65 times as long as propodus, with row of 11 robust setae along flexor margin, plus 2 ungues, more proximal much stouter than distal. Pereopod 3 ischium with two spines distally on extensor margin; merus 0.84 times length of pereopod 2 merus, 3.5 times as long as wide, with row of c. 13 ob-lique spines along extensor margin, row of spinules laterally and with three prominent spines distally on flexor margin, smaller ones proximally; carpus with seven sharp spines along extensor margin; propodus 0.71 times as long as merus, 3.5 times as long as wide, with row of eight robust setae along flexor margin plus pair dis-tally, with clusters of long setae along extensor margin; propodus three dactylus 0.68 times as long as propodus, with row of eight or nine robust setae along flexor margin, plus 2 ungues, more proxi-mal much stouter than distal. Pereopod 4 ischium with two obso-lete spines on extensor margin; merus 0.67 times length of pereopod 2 merus, 2.8 times as long as wide, with row of c. 12 ob-lique spines along extensor margin, row of spinules laterally and with three prominent spines distally on flexor margin, smaller ones proximally; carpus with c. six sharp spines along extensor margin; propodus 0.92 times as long a merus, 3.6 times as long as wide, with row of eight robust setae along flexor margin plus pair dis-tally, with clusters of long setae along extensor margin (longer
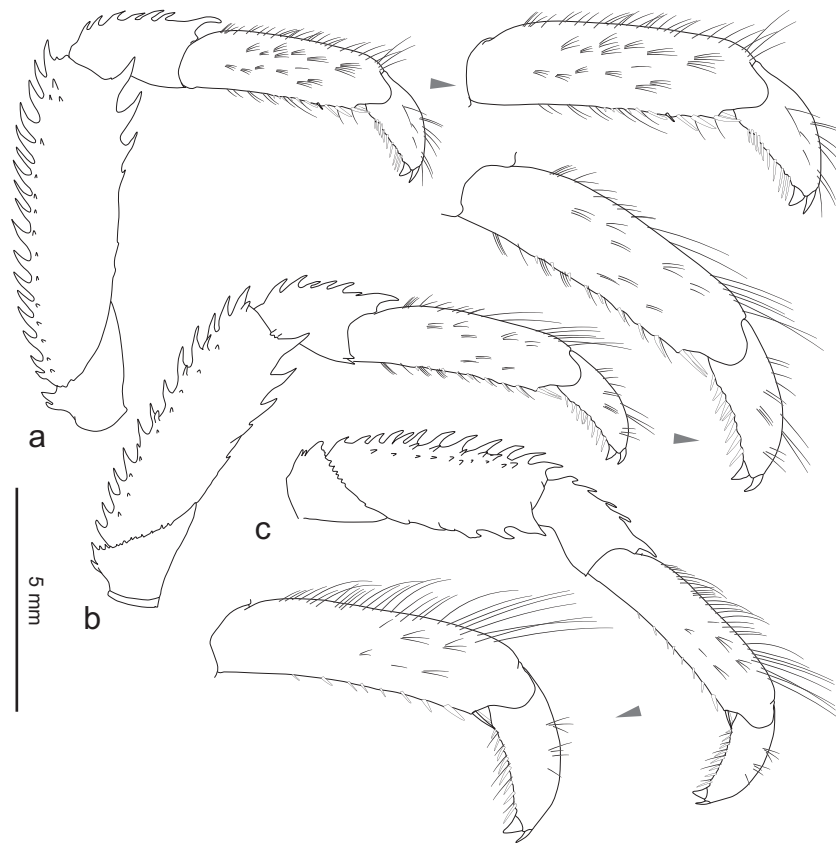
Fig. 7. *Uroptychus naso* Van Dam, 1933. (a–c) Right pereopods 2–4 with terminal articles in detail. All from syntype, ZMA, *Siboga* stn 253.

than on pereopod 3); dactylus 0.7 times as long as propodus, dactylus ornamentation as in pereopods 2 and 3.

Male pleopod 2 (gonopod 2) endopod, posterior margin evenly curved, anterior projection broad, rounded-truncate, setose; exopod distally rounded, without distal setae.

Color in life: carapace with pale middorsal stripe running from gastric region and tapering to abdominal somite 4; pereopods 2–4 orangish with paler transverse bands on ends of meri, carpi and propodi (photo T.Y. Chan).

Maximum total length, male 18.3 mm, female 17.9 mm.
Ovum diameter 1.1–1.2 mm.

4.1.4. Distribution

Southern Japan; East China Sea (Baba, 1969); Taiwan (Wu et al., 1998 (1997)); Philippines; Indonesia (Baba, 1988; Van Dam, 1933, 1939, 1940); northern Western Australia. Latitudinal range: 32°N–15°S. Lower shelf to upper continental slope, 128–440 m depth.

4.1.5. Remarks

U. naso is distinguished from *U. cyrano* and *U. pinocchio* by its generally orange color with middorsal whitish band on the carapace and abdomen. It is the only one of these three species in which the setation of the propodus of pereopod 2 is the same as pereopods 3 and 4. The carapace of *U. naso* is broader than of the other species (1.4–1.5 times as long as wide vs. 1.7–1.9 in the other species) and appears flatter. The rostrum is strongly depressed anteriorly while it is directed horizontally in the others. The carapace gives the appearance of having fewer and more widely spaced lateral branchial spines than the other two. This feature is variable and the difference difficult to quantify. The dactylus of the cheliped has only one tooth on the cutting edge, two in the other species, and is generally smooth on the upper surface.

Within *U. naso,* individuals belonging to Asian populations (mitochondrial clades I + II) were morphologically identical to individuals from NW Australia (mitochondrial clade III; Figs. 1–3) corroborating the 100% of genetic similarity recovered from the nuclear H3 marker. All specimens examined from these clades were highly variable in the degree and complexity of carapace spination and no repeatable difference could be detected. Males from Australia were slightly more elongate (mean tl/cw ratio of six males: 1.46; tl range, 7.5–16.8 mm) than males from Asia (mean tl/cw ratio of 13 males: 1.42; tl range, 10.2–18.6) but is unlikely to be significant given the different sizes of the individuals concerned. Differences in color pattern may support the genetic divergence but color of only one individual, from Taiwan, is known (Fig. 4a). We do not exclude the possibility that clades (I + II) and III may represent recently diverging biologically distinct yet morphologically cryptic taxa, maintained by geographic isolation. However, we are reluctant to describe another species based on mitochondrial clade III in the absence of (a) fixed morphological differences, (b) analysis of specimens from intermediate locations and (c) molecular support from a nuclear marker.

4.2. Uroptychus. cyrano sp. nov.

See Figs. 4b, 5b, 8 and 9.

4.2.1. Material examined

Holotype. Australia, WA, Near Mermaid Reef, 17°26.1′S, 120°26.1′E, 206–202 m, 20 June 2007 (stn SS05/2007 095), NMV J60841 (male 14.4 mm).

Paratypes. Australia. Collected with holotype, NMV J60848 (female, 11.5 mm). WA, off Point Leveque, 14°58.1′S, 121°40.6′E, 203–210 m,
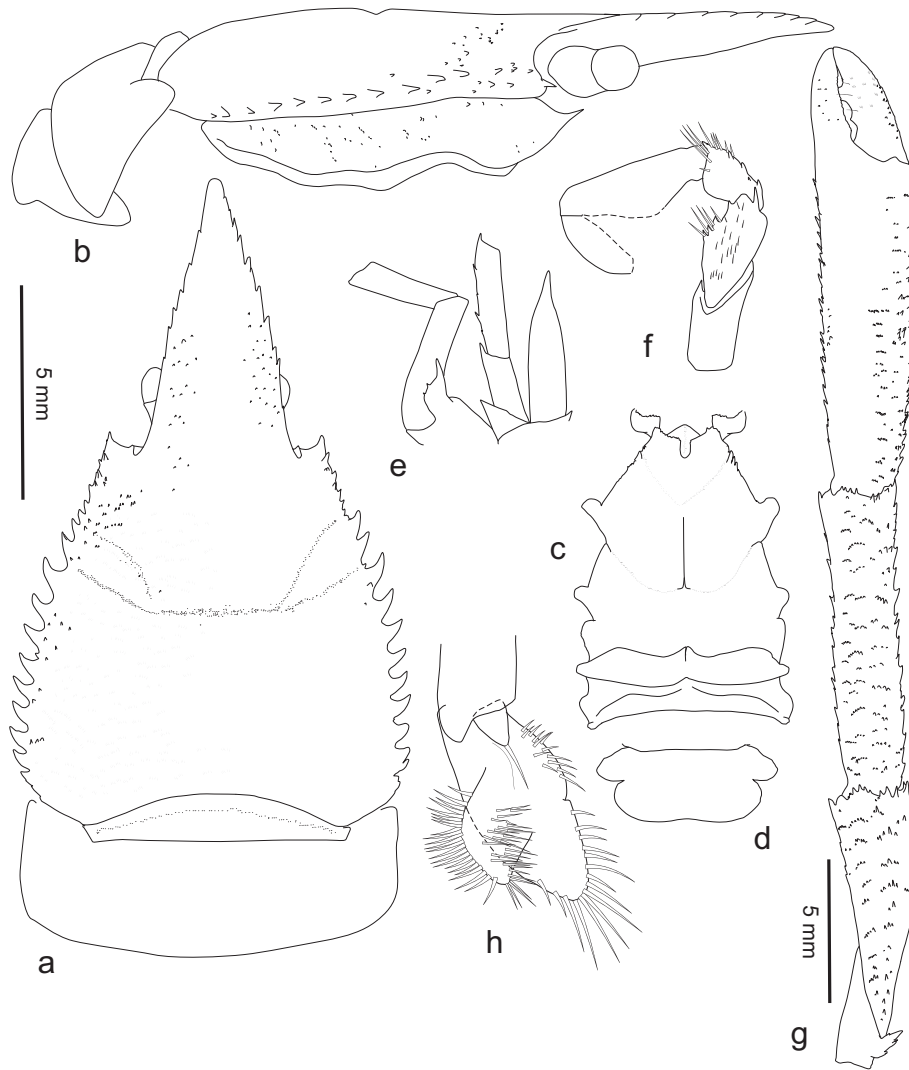
Fig. 8. *Uroptychus cyrano* new species. (a and b) Carapace and anterior abdominal somites in dorsal and lateral views; c, sternal plastron. (d) Telson. (e) Left antennule and antenna, ventral view. (f) Left maxilliped 3, lateral view. (g) Left pereopod 1, upper face in situ. (h) Left pleopod 1, lateral view. All from holotye. Pereopod 1 drawn at 2/3 scale of carapace, sternum and telson.

2 July 2007 (stn SS05/2007 142), NMV J57262 (male, 14.7 mm). Off Barrow I., 20°58.9′S, 114°43.4′E, 205–210 m, 10 June 2007 (stn SS05/2007 006), from stalked crinoid, NMV J57256 (four males 9.5–13.6 mm; two ovigerous females 10.9, 13.1 mm; juvenile 7.9 mm; plus free chelipeds). Off Point Leveque, 14°58.7′S, 121°40.2′E, 198 m, 28 June 2007 (stn SS05/2007 112), NMV J57263 (five males 7.3–8.6; four females 8.6–14.4 mm).

4.2.2. Description

Carapace moderately convex from side to side, total length (tl.) 1.74 times greatest width (cw.) (range, 1.62–1.89); distance between antennal spines (aw.) 0.59 times greatest width (cw.). Rostrum narrowly triangular, with shallow groove in dorsal midline, with rounded ventral ridge, directed horizontally anteriorly, length 0.4 times total length; dorsal surface with tubercles except in midline; lateral margin with 6–10 blunt teeth along distal two-thirds. Cervical groove at about midlength of carapace, deep medially (indistinct cervical groove and groove between anterior and posterior branchial regions laterally). Carapace covered with low tubercles, most with two or more microtubercles, strongest on anterior and posterior branchial regions and posterior to cervical groove, with transverse rows of 2–4 setules; frontal margin transverse (with small spine at midpoint); antennal spine sharp, well produced;

anterolateral margin irregularly covered with short spines; branchial margin strongly convex; anterior branchial margin with two similar spines in tandem; posterior branchial margin with nine strong similar spines, evenly spaced, intermediate spaces U-shaped, last two spines obscurely dentate. Pterygostomial flap irregularly covered with small tubercles, anterior margin with prominent upturned spine.

Sternal plastron (sternites 3–7) 1.6 times as long as wide, parallel-sided over most of length; excavated sternum rounded anteriorly, with sharp midventral ridge; sternite three slightly depressed relative to sternite 4, anterior margin excavate, with U-shaped median sinus (sinus obscurely dentate), lateral margin rounded anterolaterally, irregularly denticulate laterally, surface smooth; sternite four anterior margin 0.6 times as wide as posterior margin, anterolaterally angled, surface moderately rugose.

Abdominal somites smooth (except for transverse granular ridge on somite 1); tergites rounded anteriorly and posteriorly.

Telson 0.4 times as long in midline as greatest width; anterior section 0.45 times as long as midline length; anterolateral lobes projecting beyond posterolateral lobes, broadly rounded to subtly truncate, setose; posterior margin shallowly excavate, evenly setose.

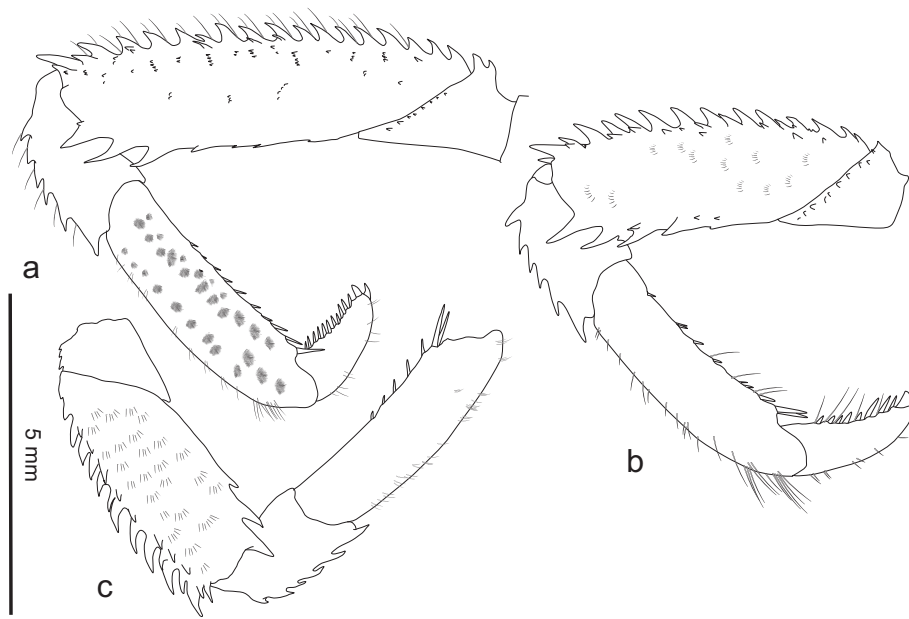Eyestalk 0.33 times length of rostrum; cornea globular, pigmented.

Fig. 9. *Uroptychus cyrano* new species. (a–c) Left pereopods 2–4. All from holotype.

Antennule article one with laterodistal triangular scale. Antenna article two with short distolateral spine; articles 3–5 with distomesial spines on all articles (article 5 with 2–3 mesial spines); article 5, 2.1 times as long as article 4; antennal scale not quite reaching to end of lateral margin of article 5, 4.3 times as long as wide, lateral margin without spines.

Maxilliped 3 merus with 1 distolateral spines, four lateral marginal spines; carpus with five spines along extensor margin.

Pereopod 1 of adult male two times as long as carapace (max.), female two times as long as carapace (max.), with scattered setae, especially on fingers; ischium with prominent complex thorn-like projection on upper margin; merus with blunt spines in row along extensor margin, with transverse rows of spines on upper face, and with only obscure teeth on flexor margin; carpus 1.1 times as long as ischium, with numerous oblique spines, arranged in short transverse rows, along extensor margin, with transverse rows of 2–6 spinules, on upper face, and with oblique spines, arranged in short transverse rows, along flexor margin; propodus 1.3 times as long as carpus, width at base of fingers 1.6 times distal width of carpus in adult, with transverse rows of oblique spines along extensor margin and rows of spinules on upper surface and with about 20 spines in uneven longitudinal row along flexor margin, cutting edge of fixed finger denticulate, concave over central half; dactylus 0.37 times as long as total length of propodus, upper margin spinulose, setose, with two teeth on cutting edge, cutting edge with proximal triangular tooth and distal truncate tooth.

Pereopods 2–4 diminishing in relative length anterior to posterior (80%), with strongly spinose ischium–carpus and with scattered setae. Pereopod 2 ischium with two spines distally on extensor margin; merus 0.44 times as long as total length of carapace, four times as long as broad, with row of c. 17 oblique spines along extensor margin, row of few smaller spines and transverse rows of spinules laterally and with three prominent spines distally on flexor margin, smaller ones proximally; carpus with six sharp spines along extensor margin; propodus 0.6 times as long as merus, 3.3 times as long as wide, with row of nine robust setae along flexor margin plus pair distally, with clusters of long setae on extensor margin and with irregular rows of dense tufts of short setae on mesial and lateral faces; dactylus 0.5 times as long as propodus, with row of 11 robust setae along flexor margin, plus

2 ungues, more proximal much stouter than distal. Pereopod 3 ischium with one spine distally on extensor margin; merus 0.78 times length of pereopod 2 merus, 3.1 times as long as wide, with row of c. 13 oblique spines along extensor margin, row of spinules laterally and with three prominent spines distally on flexor margin, smaller ones proximally (or 4); carpus with six sharp spines along extensor margin; propodus 0.79 times as long as merus, four times as long as wide, with row of eight robust setae along flexor margin plus pair distally, with clusters of long setae along extensor margin; propodus three dactylus 0.6 times as long as propodus, with row of 8 or 9 robust setae along flexor margin, plus 2 ungues, more proximal much stouter than distal. Pereopod 4 ischium with obsolete teeth on extensor margin; merus 0.64 times length of pereopod 2 merus, 2.6 times as long as wide, with row of c. 12 oblique spines along extensor margin, row of spinules laterally and with three prominent spines distally on flexor margin, smaller ones proximally; carpus with c. six sharp spines along extensor margin; propodus 0.9 times as long a merus, 3.3 times as long as wide, with row of five robust setae along flexor margin plus pair distally, with clusters of long setae along extensor margin (longer than on pereopod 3); dactylus ornamentation as in pereopods 2 and 3.

Male pleopod 2 (gonopod 2) endopod, posterior margin with broad proximal lobe, anterior projection broad, rounded-truncate, setose; exopod tapering to rounded apex, with 1 distal seta.

Color in life: carapace with two pale orangish longitudinal bands running from orbit to anterior abdominal somites, midline and lateral margins of carapace and abdominal somites off-white; pereopods off-white (photo K. Gowlett-Holmes).

Maximum total length, male 14.4 mm, female 14.7 mm.
Ovum diameter 0.6 mm.

4.2.3. Distribution
Northern Western Australia, 15°S–21°S, upper continental slope, 191–210 m depth.

4.2.4. Etymology
For Savinien de Cyrano de Bergerac (1619–1655), French soldier, satirist and playwright best remembered for his semi-autobiographic works of fiction in which he is featured with a large nose.

4.2.5. Remarks

U. cyrano shares with *U. pinocchio* a similar color pattern, generally whitish with two longitudinal orange bands on the carapace and abdomen. The carapace of both is narrower than in *U. naso* (see above) and is generally more barrel-shaped or convex dorsally (compare lateral views) and lacks the depressed rostrum. The two species also both possess differentiated setation on the propodus of pereopod 2, rows of tufts of short setae on the mesial and lateral faces. Both have two teeth on the cutting edge of the dactylus of the cheliped and spinules on the upper edge. *U. cyrano* has nine lateral branchial spines, the intervening spaces narrowly U-shaped, more evenly spaced than the seven branchial spines in *U. pinocchio* in which they are more closely spaced posteriorly. The lateral teeth of the rostrum of *U. cyrano* extend along the distal two-thirds whereas in *U. pinocchio* they are confined to the distal half.

U. cyrano is represented by clades IV and V on Figs. 1–3.

4.3. Uroptychus. pinocchio sp. nov.

Figs. 4c and d, 5c, 10 and 11.

4.3.1. Synonymy

Uroptychus naso; Van Dam (1939: p. 402–403 (part); Baba (1969, pp. 42–45 (part), Figs. 1, 2b; Baba et al (2008: 37 (part), color Fig. 1F; Baba et al. (2009: p. 47–48 (part), color Fig. 39.

4.3.2. Material examined

Holotype. Philippines, 14°1′N, 120°17′E, 184–186 m, 1980 (MUSORSTOM 2 stn CP2), MNHN Ga6232 (male, 13.2 mm).

Paratypes. Philippines, 14°02.2′N, 120°18.1′E, 202–184 m, 1976 (MUSORSTOM stn 61), MNHN Ga6230 (male, 13.2 mm). 14°0′N, 120°17′E, 170–187 m, 1980 (MUSORSTOM 2 stn CP51), MNHN Ga-6234 (one ovigerous female, damaged but complete, 14.9 mm; one female with *Sacculina* externa, 10.9 mm).

Other material.
Japan. W coast of Kyushu, 32°10′N, 128°20′E, 189 m, Schönau colln, 1898, ZMUC CRU-20208 (male, 16.5 mm). S of Goto I., 32°25′N, 128°52′E, 225 m, Suenson colln, 10 Nov 1911, ZMUC CRU-20226 (ovigerous female, 13.4 mm). 19 km W of Nagasaki, 32°02′N, 128°45′E, 198 m, Suenson colln, 1898, ZMUC CRU-20225 (male, 14.2 mm). Hirado Strait, Nagasaki, 32°10′N, 128°20′E, 189 m, Suenson colln, 1900, ZMUC CRU-11200 (male, 9.2 mm).
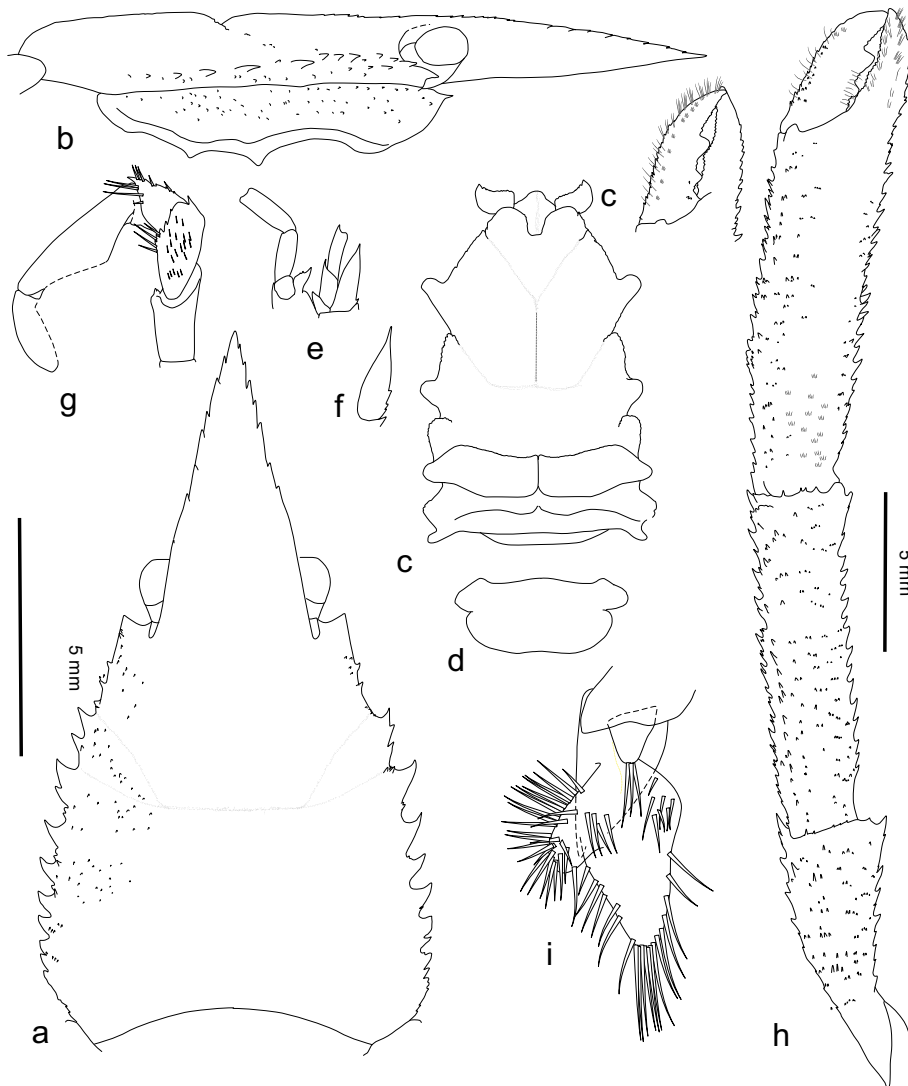*Taiwan.* Aodi, 27 Mar 2000, NTOU A00975 (male, 12.7 mm).

Fig. 10. *Uroptychus pinocchio* new species. (a and b) Carapace in dorsal and lateral views. (c) Sternal plastron. (d) Telson. (e) Left antennule and antenna, ventral view. (f) Antennal scale. (g) Left maxilliped 3, lateral view. (h) Left pereopod 1, upper face in situ. (i) Left pleopod 1, lateral view. (a–e and g–i) From holotye. (f) From MNHN Ga-6234. Pereopod 1 drawn at 2/3 scale of carapace, sternum and telson.
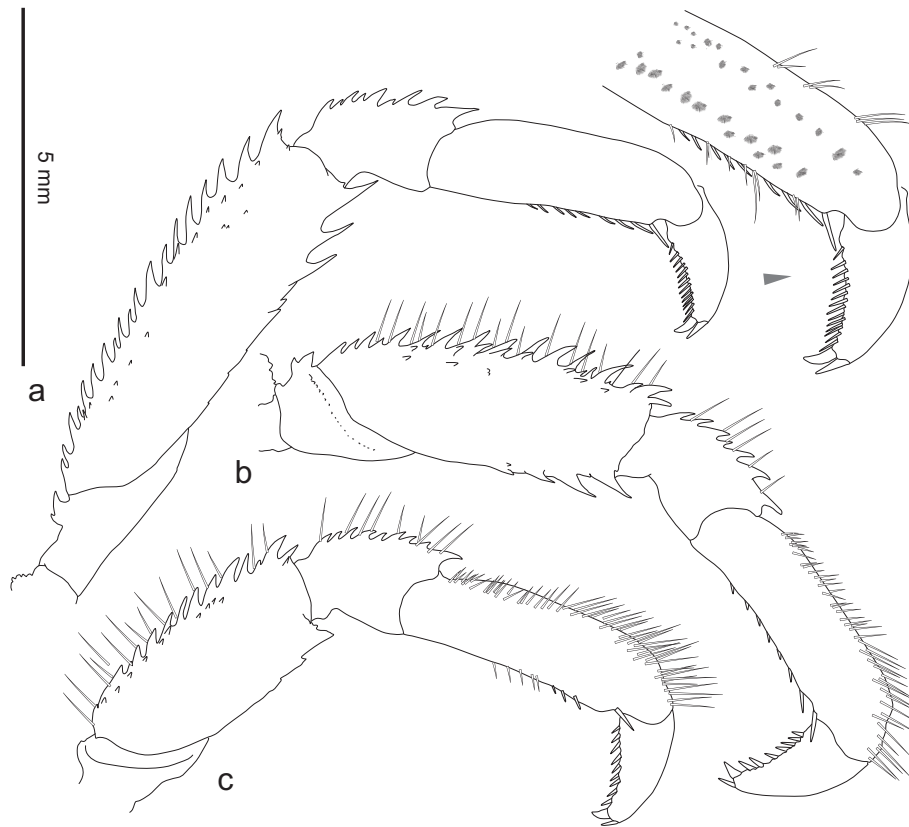
Fig. 11. *Uroptychus pinocchio* new species. (a–c) Left pereopods 2–4. All from holotype.

4.3.3. Description

Carapace moderately convex from side to side, total length (tl.) 1.72 times greatest width (cw.) (ranges 1.55–1.86); distance between antennal spines (aw.) 0.57 times greatest width (cw.). Rostrum narrowly triangular, with shallow groove in dorsal midline, with rounded ventral ridge, directed horizontally anteriorly, length 0.4 times total length; dorsal surface with tubercles except in midline; lateral margin with 7–9 blunt teeth along distal half. Cervical groove at about midlength of carapace, deep medially (indistinct cervical groove and groove between anterior and posterior branchial regions laterally). Carapace covered with low tubercles, most with 2 or more microtubercles, strongest on anterior and posterior branchial regions and posterior to cervical groove, with transverse rows of 2–4 setules; frontal margin transverse (with small spine at midpoint); antennal spine sharp, well produced; anterolateral margin irregularly covered with short spines; branchial margin strongly convex; anterior branchial margin with two similar spines in tandem (usually with a third applied to the second); posterior branchial margin with 6–7 strong spines, more prominent and more widely spaced anteriorly, obscurely differentiated posteriorly, intermediate spinules usually visible, and dentate over most posterior fifth. Pterygostomial flap irregularly covered with small tubercles, anterior margin with prominent upturned spine or produced as sharp triangle.

Sternal plastron (sternites 3–7) 1.2 times as long as wide, parallel-sided over most of length; excavated sternum rounded anteriorly, with sharp midventral ridge; sternite 3 slightly depressed relative to sternite 4, anterior margin excavate, with U-shaped median sinus (gaping), lateral margin rounded anterolaterally, irregularly denticulate laterally, surface moderately rugose;

sternite 4 anterior margin 0.64 times as wide as posterior margin, anterolaterally angled, surface smooth.

Abdominal somites smooth (except for transverse granular ridge on somite 1); tergites rounded anteriorly and posteriorly.

Telson 0.4 times as long in midline as greatest width; anterior section 0.45 times as long as midline length; anterolateral lobes projecting beyond posterolateral lobes, broadly rounded to subtly truncate, setose; posterior margin shallowly excavate, evenly setose.

Eyestalk 0.26 times length of rostrum; cornea globular, pigmented.

Antennule article 1 with laterodistal triangular scale; article 3, 2.8 times as long as wide. Antenna article 2 with short distolateral spine; articles 3–5 with distomesial spines on all articles; article 5, 1.4 times as long as article 4; antennal scale not quite reaching to end of lateral margin of article 5, three times as long as wide, lateral margin with small spine or without spines.

Maxilliped 3 merus with one distolateral spines, five lateral marginal spines; carpus with six spines along extensor margin (irregular).

Pereopod 1 of adult male 2.8 times as long as carapace (max.), female 2.2 times as long as carapace (max.), with scattered setae, especially on fingers; ischium with prominent complex thorn-like projection on upper margin; merus with blunt spines in row along extensor margin, with transverse rows of spines on upper face, and with only obscure teeth on flexor margin; carpus 1.3 times as long as ischium, with numerous oblique spines, arranged in short transverse rows, along extensor margin, with transverse rows of 2–6 spinules, on upper face, and with oblique spines, arranged in short transverse rows, along flexor margin; propodus 1.3 times as long as carpus, width at base of fingers 1.6 times distal width of carpus in adult, with transverse rows of oblique spines along extensor mar-

gin and rows of spinules on upper surface and with about 20 spines in uneven longitudinal row along flexor margin, cutting edge of fixed finger denticulate, concave over central half; dactylus 0.34 times as long as total length of propodus, upper margin spinulose, setose, with two teeth on cutting edge, cutting edge with proximal rounded tooth and distal triangular tooth.

Pereopods 2–4 diminishing in relative length anterior to posterior (80%), with strongly spinose ischium–carpus and with scattered setae. Pereopod 2 ischium with 2 spines distally on extensor margin; merus 0.44 times as long as total length of carapace, 3.7 times as long as broad, with row of c. 17 oblique spines along extensor margin, row of few smaller spines and transverse rows of spinules laterally and with three prominent spines distally on flexor margin, smaller ones proximally; carpus with nine sharp spines along extensor margin; propodus 0.57 times as long as merus, 3.2 times as long as wide, with row of eight sets or 1 or 2 robust setae along flexor margin plus pair distally, with clusters of long setae on extensor margin and with two irregular rows of dense tufts of short setae on mesial and lateral faces; dactylus 0.61 times as long as propodus, with row of 14 robust setae along flexor margin, plus 2 unges, more proximal much stouter than distal. Pereopod 3 ischium with two spines distally on extensor margin; merus 0.8 times length of pereopod 2 merus, 3.2 times as long as wide, with row of c. 13 oblique spines along extensor margin, row of spinules laterally and with three prominent spines distally on flexor margin, smaller ones proximally; carpus with seven sharp spines along extensor margin; propodus 0.7 times as long as merus, three times as long as wide, with row of 8 robust setae along flexor margin plus pair distally, with clusters of long setae along extensor margin; propodus 3 dactylus 0.6 times as long as propodus, with row of eight or nine robust setae along flexor margin, plus 2 ungues, more proximal much stouter than distal. Pereopod 4 ischium without teeth on extensor margin; merus 0.61 times length of pereopod 2 merus, 2.3 times as long as wide, with row of c. 12 oblique spines along extensor margin, row of spinules laterally and with three prominent spines distally on flexor margin, smaller ones proximally (obsolete); carpus with c. nine sharp spines along extensor margin; propodus 0.96 times as long a merus, 3.3 times as long as wide, with row of three robust setae along flexor margin plus pair distally, with clusters of long setae along extensor margin (longer than on pereopod 3); dactylus 0.64 times as long as propodus, dactylus ornamentation as in pereopods 2 and 3.

Male pleopod 2 (gonopod 2) endopod, posterior margin with broad proximal lobe, anterior projection narrow, rounded distally, setose; exopod tapering to rounded apex, with three distal setae.

Color in life: carapace with two bright brick-red or orangish longitudinal bands running from orbit to anterior abdominal somites, midline and lateral margins of carapace and abdominal somites off-white-yellowish; pereopods brick-red with distal articles of pereopods 3 and 4 bluish (photos by T.Y. Chan differ slightly).

Maximum total length, male 16.4 mm, female 14.9 mm.

Ovum diameter 0.8 mm.

4.3.4. Distribution

SW Japan (Baba, 1969; Van Dam, 1939); Taiwan (Baba et al., 2009a); Philippines. Latitudinal range: 35°N–14°N. Lower shelf, upper continental slope, 153–225 m.

4.3.5. Etymology

For Pinocchio, a wooden puppet that dreamt of becoming a real boy in the 1883 novel *Le avventure di Pinocchio* by Carlo Collodi. Pinocchio's nose grew longer when he told lies.

4.3.6. Remarks

Van Dam (1939) assigned four males and two females from Japan to *U. naso* of which we have seen four belonging to *U. pinocchio* and

only one to *U. naso*. Baba (1969) commented on differences in the setation of the propodus of pereopod 2 between females from Tosa Bay, Japan and a male from the East China Sea. His illustration of male pleopods are more likely from *U. pinocchio*. The specimens on which he commented, originally lodged in the Zoological Laboratory, Faculty of Agriculture, Kyushu University, and transferred to the Kitakyushu Museum of Natural History, Kitakyushu, cannot now be found (M. Shimomura, pers. comm.). Baba et al. (2009a) remarked again on the setation of pereopod 2 in the specimen from Aodi which we have examined. We are able to confirm that the setation is not locality- or sex-dependent as he questioned but is a real difference between *U. pinocchio* and *U. naso*. In *U. naso*, setae are arranged in more or less transverse rows, especially along the upper margin where they are longer than laterally. In *U. pinocchio*, and in *U. cyrano*, long setae along the upper margin are few but both lateral and mesial faces bear dense clusters of short setae in uneven rows. Similar clusters occur on the dactylus of pereopod 1. See above for further differences between this species and *U. naso* and the more similar *U. cyrano*.

5. Discussion

5.1. Morphological and molecular delineation of species

The combination of mitochondrial and nuclear molecular phylogenies with morphology indicated that the tropical species complex *U. naso* sensu lato consists of several mutually monophyletic mitochondrial ESUs that we interpret as three biologically distinct species. Mitochondrial clades (I + II) and III represent two genetically distinct yet morphologically identical mitochondrial lineages. Specimens belonging to these clades share identical nuclear H3 sequences and it is concluded that all belong to biological species *U. naso* sensu stricto. Individuals belonging to mitochondrial clades (I + II) and III are morphologically and genetically distinct from individuals of mitochondrial clades IV and V which are described as *U. cyrano* sp. nov. A single 16S sequence (#178) obtained from one specimen from Aodi, Taiwan, differed significantly from sequences of individuals from clades I + II (mean *p* distance = 1.4%, 2% and 4.4% from individuals of clades (I and II), III and (IV and V) respectively; results from the 16S phylogeny, data not shown) and belongs to a second new species, *U. pinocchio* sp. nov.

These three species are morphologically distinctive within *Uroptychus* and would appear to be a monophyletic clade. Until now, variation in setation of pereopod 2 (Baba, 1969) and different color patterns (Baba et al., 2009) have not been questioned or dismissed as specific characters. Here, these differences and other morphological features support genetic divergence between ESUs revealed by molecular data.

5.2. Phylogeography of U. naso

Genetic discontinuities within species are often associated with geographical patterns of distribution and may be associated with specific differences in morphology (Anker, 2007; Caputi et al., 2007; Rhyne and Lin, 2006). Hidden genetic diversity however, is not necessarily accompanied by morphological changes due to homoplasy (Bickford et al., 2007 and references therein). Mitochondrial clades I and II of *U. naso* are genetically and geographically distinct from clade III (Fig. 2a and Table 3) but could not be separated morphologically. Mitochondrial clade I is formed by four samples from Taiwan whilst haplotypes forming clade II have been obtained from three individuals in the same sample taken in deeper water in the Philippines. Individuals belonging to clade III occur in NWA. This clade was strongly supported by differences in COI and 16S gene regions as well as with resolved vs. unresolved positions of the Histone 3 gene compared to clades I + II (Fig. 2b

and c). Because individuals from clades I + II and III do not occur in sympatry, we assume the nuclear shared base pairs positions to be the result of incomplete lineage sorting due to slow convergent evolution of unsorted ancestral polymorphisms rather than ongoing hybridization or introgression between hybrids (Combosch et al., 2008; van Oppen et al., 2001). In this study, genetic data have been produced from widely geographically separated specimens. Yet, we know the species exists in intermediate regions (i.e. Indonesia). Following comparison of all material with the Indonesian syntypes, clade III is here interpreted as a genetically isolated population of *U. naso* rather than a new, reproductively isolated species.

5.3. Phylogeography of U. cyrano and U. pinocchio

Sister mitochondrial clades IV and V shared the same morphological features and identical nuclear genotypes but distinct mitochondrial haplotypes. Individuals belonging to these clades are found in sympatry on the WA continental shelf at around 200 m depth between 15°S and 21°S and likely constitute the same biological species. At the northern end of its range, *U. cyrano* co-occurs with *U. naso* mitochondrial clade III but it was not encountered in southern Western Australia by Poore et al. (2008). The similarities in morphology of *U. cyrano* and *U. pinocchio* suggest that these are sister species. Yet, we have limited material to support or contradict this hypothesis. Available material of *U. cyrano* and of *U. pinocchio* are geographically widely separated (NWA and the Philippines). Whether or where these species occur in sympatry, is unknown.

5.4. Sequencing of difficult templates

Unfortunately, we were unable to produce mitochondrial sequences from two individuals of *U. naso* from Indonesia (a syntype and ZMUC CRU-11335) and one of *U. pinocchio* from Japan (ZMUC CRU-20208). These specimens were probably formalin-fixed and could be characterized only by the sole Histone 3 gene. The PCR amplification problems were mainly related to the difficulties in extracting sufficient quality and quantity of DNA. Additionally, the scarce amount of material prevented us from using the DNA extraction protocols suitable for formalin-preserved tissues that require large amount (g) of starting tissue (e.g., Klanten et al., 2003). In a preliminary cladogram based on the H3 Histone sequences, these specimens clustered in a sister clade to *U. cyrano*. However, given the conservative nature of the marker and the difficulties encountered in amplification we must discount this result. Overall, Histone genes exhibit an acceptable level of resolution power for phylogenetic inference in crustaceans (Malay and Paulay, 2010). In addition, histones are represented by short DNA sequences, highly repeated in eukaryotic genomes and organized into clusters (Maxson et al., 1983). For these reasons these genes may represent an easy-to-amplify yet informative marker at the species level, suitable for difficult templates such as DNA obtained from tissues previously preserved in formalin.

5.5. Phylogenetic inference

The DNA regions used in this study are known to be suitable in inferring phylogenetic and phylogeographic patterns at the inter- and intra-specific levels with the mitochondrial markers being the most appropriate for cryptic species identification because of the fast mutation rate, quick lineage-specific substitution fixation and small effective population size (e.g., Cabezas et al., 2008, 2009; Machordom and Macpherson, 2004; Malay and Paulay, 2010; Seidel et al., 2009). In our study, intra- and inter-specific genetic divergence was similar in magnitude to the ones reported in munidid species using the same mitochondrial marker systems (Machordom and Macpherson, 2004) and in species of the hermit crab genus *Calcinus* (Diogenidae) using the Histone 3 gene (Malay and Paulay, 2010). H3 was successful in testing hypotheses of ancient hybridization, introgression or incomplete lineage sorting among undiscovered cryptic lineages by observing incongruence in the topology between mitochondrial and nuclear tree topologies (Sota, 2002; Sota and Vogler, 2001; Ting, 2007). We did not encounter topological incongruence between markers in our study. The sequence information gathered from the Histone 3 gene therefore helped to suggest in which cases a biological species concept could be assumed.

5.6. Historical biogeography and divergence time estimates

Molecular phylogenies and approximations of divergence dates among cryptic species and mitochondrial clades are consistent with a Tethyan MRCA for *U. naso* and *U. cyrano* from Palaeocene to early Eocene (60–50 MYA), probably of Indo-west Pacific origin. The latter region borders an archipelago of islands comprising Japan in the north, Taiwan, the Philippines, Papua New Guinea and Indonesia separated by shallow seas (Fig. 1). Squat lobsters of the *U. naso* complex are confined to the 150–400 m depth range near the edge of this shallow shelf. This continental margin is continuous along the entire WP and Indian Ocean; it represents a major center of evolutionary origin of species that radiate mainly from the East Indies (Briggs, 2005) and is a center of biodiversity for decapods and brachyurans (Feldmann and Schweitzer, 2006; Ng et al., 2008). It is therefore not surprising that genetically distinct populations of *Uroptychus,* or other squat lobster species, occur throughout this region or at least within the range of 35°N to 15°S.

Sharp genetic breaks have often been described among populations of terrestrial plant and animal species separated by Wallace's line into Asian and Australian partitions (Schulte et al., 2003 and references therein). On the other hand, similar phylogeographic patterns have been observed for marine invertebrate species distributed on either side of Huxley's line, a modification of Wallace's line (de Bruyn et al., 2004; Huxley, 1868; Lourie and Vincent, 2004). Furthermore, an invisible marine equivalent of Wallace's line, localized along the Java and Flores Seas, has been recently hypothesised as responsible for low connectivity and population fragmentation of corals within a few 100 km (Barber et al., 2000, 2002). Our phylogenies, inferred from individuals collected along the western Pacific side of Huxley's line indicate: (a) the presence of two genetically distinct cryptic species, *U. naso* and *U. cyrano* sp. nov. (mean COI *p* distance = 15.7%) and b) a second major genetic break within *U. naso* (mean COI *p* distance = 3.25%) due to fragmentation between NWA (mitochondrial clade III;) and SWP populations (mitochondrial clades I and II; Fig. 1). These levels of genetic divergence are associated with geographically predefined populations and are partitioned across a south to north cline along Huxley's line rather than an east to west Indian-Pacific ocean break. Estimated divergence dates are consistent with a round of secondary cladogenesis events beginning in early Miocene, responsible for the geographically associated genetic split among *U. naso* populations (Fig. 3). Speciation and fragmentation of populations within *U. naso* can be therefore attributed either to Wallace's marine equivalent or to the break between Asian and Australian continental plates. The same may be true for the speciation leading to sister taxa, *U. cyrano* in WA and *U. pinocchio* in the NW Pacific.

The collision between the Australian continental land mass (including Papua New Guinea) and Indonesia during Miocene (25 MYA) might have minimized the marine corridor between the Indo-Pacific water bodies, leaving the deep water of Timor Trough still able to separate the Australian and Asian continents (Hall, 1997; Poore and O'Hara, 2007). The succeeding early- to mid-Miocene was a warm period which facilitated the introduction of

warm-water species into southern Australia. East to west larval transport through the region is facilitated today by the Southeast Equatorial Current yet, genetic isolation of local shallow-water populations has also been reported (Barber et al., 2002). It seems reasonable to assume that the presence of *U. naso* mitochondrial clade III on the western Australian continental margin represents a historical event of dispersal and geographical isolation since Miocene, maintained by restrictive current flows.

6. Concluding remarks

Despite the considerable debates related to the exact position and origins of the biogeographic breaks mentioned, it is unquestionable that the composition and geographical patterns of marine and terrestrial biota are influenced by the complicated geological history of the zone (plate tectonic history of the East Indies triangle, break between ocean bodies during Pleistocene and the collision of the Australian and the Eurasian plates some 25 MY before present; Schulte et al., 2003). Information from other deep-sea invertebrates should reveal whether the aforementioned historical signatures account for a standard distribution trend of species, useful for biodiversity discovery and estimates, connectivity, conservation and sustainable use of marine resources.

References

Ahyong, S.T., Schnabel, K.E., Macpherson, E., in press. Phylogeny and fossil record of the marine squat lobsters. In: Poore, G.C.B., Ahyong, S.T., Taylor, J. (Eds.), Crustacean Issues vol. 20: The Biology of Squat Lobsters. CSIRO Publishing, Melbourne and CRC Press, Boca Raton (Chapter 4).

Aljanabi, S.M., Martinez, I., 1997. Universal and rapid salt-extraction of high quality genomic DNA for PCR-based techniques. Nucleic Acids Research 25, 4692–4693.

Anker, A., 2007. *Pseudalpheopsis guana* gen. nov., sp. nov. (Crustacea: Decapoda), a new alpheid shrimp from the British Virgin Islands, Caribbean Sea. Zoological Studies 46, 428–440.

Baba, K., 1969. Chirostylids and galatheids from dredgings and trawlings operated in the East China Sea by the Japanese Fisheries Research Vessel Kaiyo Maru in 1967. OHMU 2, 41–57.

Baba, K., 1988. Chirostylid and galatheid crustaceans (Decapoda: Anomura) of the "Albatross" Philippine Expedition, 1907–1910. Researches on Crustacea, Special Number 2, 1–203.

Baba, K., 2005. Deep-sea chirostylid and galatheid crustaceans (Decapoda: Anomura) from the Indo-West Pacific, with a list of species. Galathea Report 20, 1–317.

Baba, K., Lin, C.-W., 2008. Five new species of chirostylid crustaceans (Crustacea: Decapoda: Anomura: Chirostylidae) from Taiwan. Zootaxa 1918, 1–24.

Baba, K., Macpherson, E., Poore, G.C.B., Ahyong, S.T., Bermudez, A., Cabezas, P., Lin, C.-W., Nizinski, M., Rodrigues, C., Schnabel, K.E., 2008. Catalogue of squat lobsters of the world (Crustacea: Decapoda: Anomura—families Chirostylidae, Galatheidae and Kiwaidae). Zootaxa 1905, 1–220.

Baba, K., Macpherson, E., Lin, C.-W., Chan, T.-Y., 2009. Crustacean fauna of Taiwan: squat lobsters (Chirostylidae and Galatheidae). National Taiwan Ocean University, Keelung.

Bandelt, H.J., Forster, P., Röhl, A., 1999. Median-joining networks for inferring intraspecific phylogenies. Molecular Biology and Evolution 16, 37–48.

Barber, P., Palumbi, S., Erdmann, M., Moosa, M.K., 2000. A marine Wallace's line? Nature 406, 692–693.

Barber, P., Palumbi, S., Erdmann, M.V., Moosa, K., 2002. Sharp genetic breaks among populations of *Haptosquilla pulchella* (Stomatopoda) indicate limits to larval transport: patterns, causes, and consequences. Molecular Ecology 11, 659–674.

Bickford, D., Lohman, D.J., Sodhi, N.S., Ng, P.K.L., Meier, R., Winker, K., Ingram, K.K., Das, I., 2007. Cryptic species as a window on diversity and conservation. Trends in Ecology & Evolution 22, 148–155.

Briggs, J.C., 2005. The marine East Indies: diversity and speciation. Journal of Biogeography 31, 1975–1985.

de Bruyn, M., Wilson, J.A., Mather, P.B., 2004. Huxley's line demarcates extensive genetic divergence between eastern and western forms of the giant freshwater prawn *Macrobrachium rosenbergii*. Molecular Biology and Evolution 30, 251–257.

Cabezas, P., Macpherson, E., Machordom, A., 2008. A new genus of squat lobster (Decapoda: Anomura: Galatheidae) from the South West Pacific and Indian Ocean inferred from morphological and molecular evidence. Journal of Crustacean Biology 28, 68–75.

Cabezas, P., Macpherson, E., Machordom, A., 2009. Morphological and molecular description of new species of squat lobster (Crustacea: Decapoda: Galatheidae) from the Solomon and Fiji Islans (SW Pacific). Zoological Journal of the Linnean Society 156, 465–493.

Caputi, L., Andreakis, N., Mastrototaro, F., Cirino, P., Vassillo, M., Sordino, P., 2007. Cryptic speciation in a model invertebrate chordate. Proceedings of the National Academy of Sciences of the United States of America 104, 9364–9369.

Colgan, D.J., McLauchlan, A., Wilson, G.D.F., Livingston, S.P., Edgecombe, G.D., Macaranas, J., Cassis, G., Gray, M.R., 1998. Histone H3 and U2 snRNA DNA sequences and arthropod molecular evolution. Australian Journal of Zoology 46, 419–437.

Combosch, D.J., Guzman, H.M., Schuhmacher, H., Vollmer, S.V., 2008. Interspecific hybridization and restricted trans-Pacific gene flow in the Tropical Eastern Pacific *Pocillopora*. Molecular Ecology 17, 1304–1312.

Dallwitz, M.J., Paine, T.A., Zurcher, E.J., 1999. User's guide to the DELTA system. A general system for processing taxonomic descriptions. CSIRO Division of Entomology, Canberra.

Drummond, A.J., Rambaut, A., 2007. BEAST: Bayesian evolutionary analysis by sampling trees. BMC Evolutionary Biology 7, 214.

Drummond, A.J., Ho, S.Y.W., Phillips, M.J., Rambaut, A., 2006. Relaxed phylogenetics and dating with confidence. PLoS Biology 4, e88.

Edgar, R.C., 2004. MUSCLE: multiple sequence alignment with high accuracy and high throughput. Nucleic Acids Research 32, 1792–1797.

Feldmann, R.M., 1984. *Haumuriaegla glaessneri* n. gen. and sp. (Decapoda; Anomura; Aeglidae) from Haumurian (Late Cretaceous) rocks near Cheviot, New Zealand. New Zealand Journal of Geology and Geophysics 27, 379–385.

Feldmann, R.M., Schweitzer, C.E., 2006. Paleobiogeography of Southern Hemisphere decapod Crustacea. Journal of Paleontology 80, 83–103.

Feldmann, R.M., Vega, F.J., Applegate, S.P., Bishop, G.A., 1998. Early Cretaceous arthropods from the Tlayúa Formation at Tepexi de Rodríguez, Puebla, Mexico. Journal of Paleontology 72, 79–90.

Felsenstein, J., 1985. Confidence limits on phylogenies: an approach using the bootstrap. Evolution 39, 783–791.

Folmer, O., Black, M., Heoh, W., Lutz, R.A., Vrijenhoek, R., 1994. DNA primers for the amplification of mitochondrial cytochrome C oxidase subunit I from diverse metazoan invertebrates. Molecular Marine Biology and Biotechnology 3, 294–299.

Hall, R., 1997. Cenozoic plate tectonic reconstructions of SE Asia. Geological Society of London, Special Publications 126, 11–23.

Hall, T.A., 1999. BioEdit: a user-friendly biological sequence alignment editor and analysis program for Windows 95/98/NT. Nucleic Acids Symposium 41, 95–98.

Hillis, D.M., Huelsenbeck, J.P., 1992. Signal, noise and reliability in molecular phylogenetic analysis. Journal of Heredity 83, 189–195.

Huelsenbeck, J.P., Ronquist, F., 2001. MRBAYES: Bayesian inference of phylogenetic trees. Bioinformatics 17, 754–755.

Huxley, T.H., 1868. On the classification and distribution of the Alectoromorphae and Heteromorphae. Proceedings of the Zoological Society of London 6, 294–319.

Jakobsen, S.L., Collins, J.S.H., 1997. New Middle Danian species of anomuran and brachyuran crabs from Fakse, Denmark. Bulletin of the Geological Society of Denmark 44, 89–100.

Klanten, S., Van Herwerden, L., Howard, C.J., 2003. Acquiring reef fish DNA sequences from formalin-fixed museum specimens. Bulletin of Marine Science 73, 771–776.

Knowlton, N., 1986. Cryptic and sibling species among the Decapod crustacea. Crustacean Biology 6, 263–356.

Lourie, S.A., Vincent, C.J., 2004. A marine fish follows Wallace's Line: the phylogeography of the three-spot seahorse (*Hippocampus trimaculatus*, Syngnathidae, Teleostei) in Southeast Asia. Journal of Biogeography 31, 1975–1985.

Machordom, A., Macpherson, E., 2004. Rapid radiation and cryptic speciation in galatheid crabs of the genus *Munida* and related genera in the South West Pacific: molecular and morphological evidence. Molecular Phylogenetics and Evolution 33, 259–279.

Malay, M.C.D., Paulay, G., 2010. Peripatric speciation drives diversification and distributional patterns of reef hermit crabs (Decapoda: Diogenidae: *Calcinus*). Evolution 64, 634–662.

Maxson, R., Cohn, R., Kedes, L., Mohun, T., 1983. Expression and organization of histone genes. Annual Review of Genetics 17, 239–277.

Moritz, C., 1994. Defining "evolutionarily significant units" for conservation. Trends in Ecology & Evolution 9, 373–375.

Ng, P.K.L., Guinot, D., Davie, P.J.F., 2008. Systema Brachyurorum: part I. An annotated checklist of extant brachyuran crabs of the world. Raffles Bulletin of Zoology 17, 1–286.

Palumbi, S.R., Benzie, J., 1991. Large mitochondrial DNA differences between morphologically similar penaeid shrimp. Marine Biology and Biotechnology 1, 27–34.

Poore, G.C.B., O'Hara, T.D., 2007. Marine biogeography and biodiversity of Australia. In: Connell, S.D., Gillanders, B.M. (Eds.), Marine Ecology. Oxford University Press, pp. 177–198.

Poore, G.C.B., McCallum, A.W., Taylor, J., 2008. Decapod Crustacea of the continental margin of southwestern and central Western Australia: preliminary identifications of 524 species from FRV Southern Surveyor voyage SS10–2005. Museum Victoria Science Reports 11, 1–106.

Porter, S.C., 1989. Some geological implications of average Quaternary glacial conditions. Quaternary Research 32, 245–261.

Posada, D., Crandall, K.A., 1998. Modeltest: testing the model of DNA substitution. Bioinformatics 14, 817–818.

Rambaut, A., Drummond, A.J., 2007. Tracer v1.4. <http://beast.bio.ed.ac.uk/Tracer>.

Rhyne, A.L., Lin, J., 2006. A western Atlantic peppermint shrimp complex: redescription of *Lysmata wurdemanni* (Gibbes), description of four new species and remarks on *L. rathbunae* Chace (Crustacea: Decapoda: Hippolytidae). Bulletin of Marine Science 79, 165–204.

Schnabel, K.E., 2009. A review of the New Zealand Chirostylidae (Anomura: Galatheoidea) with description of six new species from the Kermadec Islands. Zoological Journal of the Linnean Society 155, 542–582.

Schnabel, K.E., Ahyong, S.T., 2010. A new classification of the Chirostyloidea (Crustacea: Decapoda: Anomura). Zootaxa 2687, 56–64.

Schulte, J.A., Melville, L., Larson, A., 2003. Molecular evidence of ancient divergence of lizard taxa on either side of the Wallace's line. Proceedings of the Zoological Society of London B 270, 597–603.

Schweitzer, C.E., Feldmann, R.M., 2000. First notice of the Chirostylidae (Decapoda) in the fossil record and new Tertiary Galatheidae (Decapoda) from the Americas. Bulletin of the Mizunami Fossil Museum 27, 147–165.

Seidel, R.A., Lang, B.K., Berg, D.J., 2009. Phylogeographic analysis reveals multiple cryptic species of amphipods (Crustacea: Amphipoda) in Chihuahuan Desert springs. Biological Conservation 142, 2303–2313.

Sota, T., 2002. Radiation and reticulation: extensive introgressive hybridization in the carabid beetles *Ohomopterus* inferred from mitochondrial gene genealogy. Population Ecology 44, 145–156.

Sota, T., Vogler, A.P., 2001. Incongruence of mitochondrial and nuclear gene trees in the carabid beetles *Ohomopterus*. Systematic Biology 50, 39–59.

Swofford, D.L., 2002. PAUP*. Phylogenetic Analysis Using Parsimony (*and Other Methods). Version 4. Sinauer Associates, Sunderland.

Taylor, J., Ahyong, S.T., Andreakis, N., 2010. New records and new species of the munidopsine squat lobsters (Decapoda: Anomura: Galatheidae: Munidopsinae) from Australia. Zootaxa 2642, 1–18.

Thompson, J.D., Higgins, D.G., Gibson, T.J., 1994. CLUSTAL W: improving the sensitivity of progressive multiple sequence alignment through sequence weighting, position specific gap penalties and weight matrix choice. Nucleic Acids Research 22, 4673–4680.

Ting, N., 2007. Mitochondrial relationships and divergence dates of the African colobines: evidence of Miocene origins for the living colobus monkeys. Journal of Human Evolution 55, 312–325.

Van Dam, A.J., 1933. Die Chirostylidae der Siboga-Expedition. Decapoda VIII: Galatheidea: Chirostylidae. Siboga-Expéditie, 39a7, 1–46.

Van Dam, A.J., 1939. Ueber einige *Uroptychus*-Arten des Museums zu Kopenhagen. Bijdragen tot de Dierkunde 27, 392–407.

Van Dam, A.J., 1940. Anomura, gesammelt vom Dampfer Gier in der Java-See. Zoologischer Anzeiger 129, 95–104.

van Oppen, M.J.H., McDonald, B.J., Willis, B., Miller, D.J., 2001. The evolutionary history of the coral genus *Acropora* (Scleractinia, Cnidaria) based on a mitochondrial and a nuclear marker: reticulation, incomplete lineage sorting, or morphological convergence? Molecular Biology and Evolution 18, 1315–1329.

Wang, Y., 2008. Infraorder Anomura MacLeay, 1838. In: Liu, J.-Y. (Ed.), Checklist of Marine Biota of China Seas. Science Press, Qingdao, pp. 748–751.

Williams, S.T., Jara, J., Gomez, E., Knowlton, N., 2002. The marine Indo-West Pacific break: contrasting the resolving power of mitochondrial and nuclear genes. Integrative and Comparative Biology 42, 941–952.

Wu, M.F., Chan, T.-Y., Yu, H.P., 1997. On the Chirostylidae and Galatheidae (Crustacea: Decapoda: Galatheidea) of Taiwan. Annual of Taiwan Museum 40, 75–153 (1998).